HHS Public Access

Author manuscript

Nat Biomed Eng. Author manuscript; available in PMC 2022 February 25.

Published in final edited form as:

Nat Biomed Eng. 2021 January ; 5(1): 89–102. doi:10.1038/s41551-020-00674-w.

Mechanobiological Conditioning Enhances Mesenchymal Stem Cell-Induced Vascular Regeneration

Jason Lee[1], **Kayla Henderson**[1], **Miles W. Massidda**[1], **Miguel Armenta-Ochoa**[1], **Byung Gee Im**[1], **Austin Veith**[1], **Bum-Kyu Lee**[2], **Mijeong Kim**[2], **Pablo Maceda**[1], **Eun Yoon**[1], **Lara Samarneh**[1], **Mitchell Wong**[1], **Andrew K. Dunn**[1], **Jonghwan Kim**[2], **Aaron B. Baker**[1,2,3,4]

[1]University of Texas at Austin, Department of Biomedical Engineering, Austin, TX

[2]Institute for Cellular and Molecular Biology, University of Texas at Austin, Austin, TX

[3]The Institute for Computational Engineering and Sciences, University of Texas at Austin, Austin, TX

[4]Institute for Biomaterials, Drug Delivery and Regenerative Medicine, University of Texas at Austin, Austin, TX

Stem cell therapies have great promise for revolutionizing treatments for cardiovascular disease and other disorders but have not yet achieved their potential due to poor efficacy and heterogeneity in patient response. We used a high throughput mechanobiological screening system to explore a combinatorial parameter space of mechanical forces and pharmacological inhibitor to enhance mesenchymal stem cell properties for enabling vascular regeneration. Our studies revealed that treatment specific mechanical conditions combined with small molecules could dramatically increase the activation of Smad2 and Yap-mediated signaling, leading to an increased population of mesenchymal stem cells that simultaneously expressed markers associated with pericytes and endothelial cells. We found these conditioned cells had increased angiogenic activity in *in vitro* functional assays, enhanced gene expression for pericyte and endothelial phenotypes by RNA sequencing and were able to improve the formation of vasculature in models of subcutaneous implantation and hind limb ischemia. Mechanistic studies suggested these effects were mediated by a complex signaling pathway with crosstalk between EGFR family receptors, TGF-β receptor type 1 and VEGF receptor 2. Overall, our findings demonstrate that optimized mechanical and pharmacological conditioning can significantly enhance the regenerative properties of mesenchymal stem cells.

Cell based therapies have great potential for revolutionizing the treatment of diseases that are not amenable to traditional treatments. Therapies based on mesenchymal stem cells (MSCs) are particularly appealing as they are a source of autologous cells with multipotency and can be harvested from patients with relative ease. In addition, MSCs may be able to self-renew[1, 2] and have immunosuppressive properties that make them potential candidates for

Correspondence to: Aaron B. Baker, Ph.D., University of Texas at Austin, Department of Biomedical Engineering, 1 University Station, BME 5.202D, C0800, Austin, TX 78712, Phone: 512-232-7114, abbaker1@gmail.com.

autologous cellular therapeutics[3]. For cardiovascular therapies, MSCs have been explored for the treatment of myocardial infarct and peripheral ischemia[4–9]. However, these trials have not shown consistent long-term benefits to patients from MSC therapies in spite of intense investigation by many groups[10–13]. MSCs have several aspects that limit their potential for use in cell therapies. In conventional culture conditions, MSCs lose their differentiation potential and have reduced therapeutic properties after expansion[14, 15]. In addition, the isolated MSC populations have a high degree of heterogeneity, with subsets of cells that have varying degrees of potential for inducing regeneration[16, 17]. Moreover, the therapeutic potential of MSCs is altered by the health of the patient from which they are harvested. This is a major limitation as patients with advanced age, obesity, diabetes and other chronic disorders have MSCs with reduced regenerative properties[14, 15, 18–21]. Thus, those patients who would likely benefit the most from cell therapies are those who have the least regenerative MSCs. Genetic modification of MSCs could potentially address some of these issues but would also raise concerns of tumorigenicity[22]. Consequently, there is an intense interest in identifying alternative strategies for making MSCs more effective and reliable in spite of patient-to-patient differences in MSC behavior and reduced inherent regenerative capability.

The differentiation of MSCs into vascular cell types would be highly advantageous for many clinical applications including the treatment of ischemia and in tissue engineered vascular grafts. Unfortunately, there has not been consensus in the field as to what conditions induce endothelial differentiation in MSCs or even if the phenotype obtained is truly endothelial in nature[23–26]. Biophysical forces, including shear stress and mechanical stretch, have been used to condition MSCs into vascular phenotypes[27–32]. Several studies have shown that shear stress and treatments such as VEGF can lead to the expression of endothelial markers in MSCs[23, 25]. However, some studies have found contrasting results in endothelial differentiation for identical treatments or an increase in markers for vascular smooth muscle cells (vSMCs) in addition to those for endothelial cells[31–34]. Thus, it is unclear what conditions are optimal for obtaining an endothelial cell-like phenotype in MSCs. Moreover, it is unclear if enhancing endothelial or vascular phenotype also increases the effectiveness of MSC therapies.

In this work, we used a novel high throughput system for applying mechanical stretch to cultured cells to explore the ability of applied mechanical forces to enhance the regenerative properties of MSCs. Using this system, we performed a set of powerful screening assays that explored the synergy between biochemical factors, pharmacological inhibitors and biomechanical forces in conditioning MSCs into vascular cell-like phenotypes that have enhanced regenerative properties. We identified specific mechanical conditions that induce maximal activation of the Yap and Smad2/3-mediated signaling pathways in MSCs. Using a high throughput screen incorporating applied mechanical load, we also identified pharmacological inhibitors that synergistically activated these pathways. A rigorous analysis of the phenotype of the cells treated with combined mechanical conditioning and drug treatments revealed increased expression of both pericyte and endothelial markers. These optimally conditioned MSCs exhibited enhanced pericyte and endothelial behavior *in vitro*, production of angiogenic soluble factors, and increased therapeutic potential in enhancing blood vessel growth in animal models of subcutaneous implantation and hind limb ischemia.

Results

Specific types of applied mechanical load activate Smad2/3 transcription factor activity and Yap nuclear localization in mesenchymal stem cells.

Treatment with VEGF-A and TGF-β1 has been linked to differentiation of MSCs into vascular cell types and other lineages[23, 25, 35]. We recently developed a system that allows the application of mechanical stretch in a high throughput format with 576 individual culture well with mechanical load[36–38]. Using this system, we explored whether there was synergy between biochemical and mechanical stimuli to activate the transcription factors by exposing the cells to VEGF-A or TGF-β1 during mechanical loading. We transduced MSCs with lentiviruses expressing luciferase reporter constructs for Smad2/3 and selected these to obtain a stable reporter cell line. We found that low frequency mechanical loading (0.1 Hz, 5% maximal strain) activated Smad2/3 transcription while higher frequencies of loading did not (Fig. 1A). In addition, there was synergy in Smad2/3 transcription with TGF-β1 treatment and mechanical loading at 0.1 Hz, and this was suppressed by loading at 1 or 2 Hz (Fig. 1A). Using a multi-strain configuration of the device, we did a dose response to the magnitude of mechanical strain and found maximal activation of Smad2/3 in the presence of TGF-β1 and 7.5% cyclic mechanical strain (Fig. 1B). We repeated the studies under similar conditions and found that there was a maximal nuclear localization of Yap at 7.5% strain, similar to the activation of Smad2/3 (Fig. 1C-E). While we observed maximal activity of Smad2/3 in our studies at 7.5% strain, nuclear intensity of Smad2/3 increased in loads higher than 7.5% strain, implying there may be a repressive activity present towards Smad2/3 at higher strains. We then immunostained for markers of vascular lineage and found that there was an increase in the vascular smooth muscle cell (vSMC)/myofibroblast marker α-SMA at mid-level strains (Fig. 1C, F). We co-stained for integrin-linked kinase (ILK), a known suppressor of the Hippo pathway[39], but did not see a significant difference with mechanical load (Fig. 1C). The loading system uses a linear motor that allow the application of complex physiological mechanical strain waveforms including a brachial waveform that simulated the distension of the brachial artery during the cardiac cycle (Fig. 1G). We repeated loading at 0.1 Hz, 7.5% maximal strain with the sine and brachial waveforms and then immunoblotted for vascular markers. While our primary goal was to exam the effects of a broad range of mechanical forces on MSC differentiation, the brachial loading profile is mimetic of the brachial artery may simulate the forces that would be experienced by a MSC in or near to the artery stretching during the cardiac cycle. We found that there was an increase in the endothelial cell marker PECAM-1 and p-Smad2/3 and a marked reduction in α-SMA with the brachial waveform loading (Fig. 1H; Supplemental Fig. 1). In order to confirm that baseline and and lentivirus transduced MSCs retained their natural expression profile, we confirmed the MSC phenotype of the cells using flow cytometry (Supplemental Fig. 2). Additionally, we confirmed that the cells could differentiate into adipogenic and osteogenic lineages at the passage used (Supplemental Fig. 3).

High throughput drug screening assay with mechanical load identifies kinase inhibitors that enhance Smad2/3 signaling and Hippo pathway activation in synergy with mechanical load.

We next used the mechanical loading system to perform a screening assay to identify compounds that could enhance Smad and Hippo pathway activation in combination with mechanical load. We performed mechanical loading on MSCs in the 96-well format in the presence of one of 80 compounds from a kinase inhibitor library. After 24 hours, we immunostained for p-Smad2/3 and Yap/Taz, and then quantified the nuclear staining of both signaling intermediates (Fig. 2A, B; Supplemental Fig. 4-6). From this assay, we identified compounds that markedly increased both nuclear Yap and p-Smad2/3 (Fig. 2). Many of the top hits from the assay included inhibitors of the EGFR pathways (Fig. 2C). We chose the EGFR/ErbB-2/4 inhibitor N-(4-((3-chloro-4-fluorophenyl)amino)pyrido[3,4-d]pyrimidin-6-yl)2butynamide (CAS 881001–19-0) and the PKCbII/EGFR inhibitor 4,5-bis(4-fluoroanilino)phthalimide (CAS 145915–60-2) for further study based on the maximal activation of both pathways or maximal activation of the Hippo pathway, respectively. We performed immunostaining on treated MSCs from a different donor and found a weak correlation between PECAM-1/α−SMA for p-Smad2/3 (Supplemental Fig. 7A-C) and a moderate strong correlation between these markers and nuclear Yap/Taz (Supplemental Fig. 7D-F).

Brachial waveform mechanical loading and pharmacological inhibition induce a hybrid endothelial/pericyte phenotype in MSCs with enhanced angiogenic properties.

The induction of endothelial phenotype in MSCs would be advantageous in many therapeutic applications. Unfortunately, several studies of endothelial differentiation of MSCs have shown contradictory results[23, 25, 26]. Recent studies have also suggested that MSCs may be related to or identical to pericytes[40]. However, other studies do not support that pericytes have stem cell-like properties[41]. Pericyte markers in MSCs are correlated with enhanced regenerative properties in MSCs[42–45]. Many studies have been done that only look at one or two markers and conclude a phenotype of endothelial and vSMC lineage, making the true phenotype difficult to assess. To address these issues, we applied a combinatorial set of mechanical loading and biochemical/pharmacological treatments to MSCs and then assessed their phenotype with multiple markers using flow cytometry (Supplemental Fig. 8). We included in the treatments the pharmacological inhibitors identified in the high throughput screen that synergistically activated p-Smad2/3 and induce Yap/Taz nuclear localization as well as treatments from previous studies that led to vascular cell differentiation. Using a rigorous definition for endothelial cell phenotype that required expression of multiple endothelial markers, there was little endothelial lineage expressed by the cells under baseline conditions and with the treatments. Notably, VEGF did not increase the endothelial cell lineage in the MSCs, as defined by multiple markers using flow cytometry (Supplemental Fig. 9). In addition, there was only a very small proportion of cell expressing all of the marker profile of pericytes ($PECAM^-$ $CD105^-$ $VE\text{-}Cad^-$ $CD146^+$ $Nestin^+$ $PDGFR\beta^+$ cells). With brachial waveform mechanical loading, there was an increase in cells with both endothelial markers (PECAM-1, VE-Cad, and CD105) and markers for pericytes (CD146, Nestin and PDGFRβ). This population was also largely positive for NG2, suggesting a hybrid phenotype of type 2 pericytes and

endothelial cells (Supplemental Fig. 9). This EC/pericyte population was markedly increased following treatment with brachial loading and co-treatment with kinase inhibitors identified from drug screening assay to activate pSmad2/3 and Yap (Supplemental Fig. 9). To test the robustness of these findings we repeated some of the treatments in two additional donors and analyzed their marker expression using flow cytometry using mature cell lines (endothelial cells and pericytes) as standards for each phenotype (Supplemental Fig. 10). This analysis demonstrated an increase in the subpopulation with markers for endothelial cells and pericytes for MSCs treated with brachial loading and the E/E inhibitor for both donors (Fig. 3A). In addition, there was an increase in cells with the endothelial cell phenotype in MSCs treated with brachial waveform loading and E/E inhibitor (Fig. 3A), although this population was much smaller than the EC/pericyte population. At baseline the MSCs had a mid range expression of PECAM in comparison to pericytes and endothelial cells. To assess whether the MSCs expressed markers at similar levels to the mature cells lines, we compared the staining intensities within the gated populations (Supplemental Fig. 11). The level of expression of PECAM-1, CD144 and CD105 in the EC/pericyte population in the MSCs treated with brachial waveform loading and the E/E inhibitor was similar to that of mature endothelial cells. In addition, the EC/pericyte population from MSCs treated with brachial waveform loading and E/E inhibitor had similar expression of PDGFRβ, lower expression of CD146 and NG2, and higher expression of nestin in comparison to pericytes. We also analyzed the cells using a live-dead assay to exclude the possibility this population was composed of dead cells (Supplemental Fig. 12). To investigate if this population exists in the bone marrow *in vivo*, we sorted fresh bone marrow mononuclear cells and found that a small population that expressed both PECAM-1 and PDGFRβ markers (~0.046% of bone marrow mononuclear cells; Supplemental Fig. 13). However, we did not observe a population that expressed the full set of EC/pericyte markers. We did not observe cells with the full set of EC/pericyte markers. These findings suggest there may be a related phenotype in the bone marrow, but the full phenotype is not present or is very rare.

Biomechanical conditioning increases pericyte-like activity and angiogenic properties of MSCs.

We next examined whether the cells under the different conditions had increased pericyte-like behavior and pro-angiogenic activity using a tube formation assay. Conditioned media from MSCs treated with brachial loading with or without pharmacological inhibitors induced increased tube formation in endothelial cells (Fig. 3B; Supplemental Fig. 14A). We also plated the MSCs on Matrigel directly and found that there was increased formation of mature tubes at later time points (Fig. 3B; Supplemental Fig. 14B). We then mixed MSCs with endothelial cells and plated them together to examine the effect of mechanical/biochemical conditioning on inducing pericyte-like behavior in MSCs. This analysis showed that MSCs exposed to brachial waveform loading had increased tube formation in co-culture with endothelial cells (Fig. 3B; Supplemental Fig. 14C). We performed mechanical loading of MSCs with the sine and brachial waveforms (4 hours/day) and treated with pharmacological inhibitors for seven days (the compounds were not added in the final day treatment). The conditioned media from MSCs under the treatments were found to decrease endothelial cell proliferation in comparison to conditioned media from cells grown under control conditions (Supplemental Fig. 15).

We next examined the production of growth factors by MSCs under mechanical loading with co-treatment with pharmacological inhibitors following short term (24 hours) or longer term (7 days) treatment. We performed an antibody array analysis on the conditioned media from the treated cells and identified alterations in growth factor production by the MSCs after 24 hours or seven days of loading with co-treatments (Supplemental Fig. 16). We used ELISA to measure changes in the growth factors and found increases in angiotensin-1 (Ang-1) and VEGF-A with sine wave loading after 24 hours (Supplemental Fig. 17). Following seven days of loading, there was a marked increase in hepatocyte growth factor (HGF), a pro-angiogenic growth factor[46], in all of the groups treated with mechanical load (Supplemental Fig. 18). In the groups treated with brachial loading, there was also a decrease in TGF-β1, Ang-1 and Ang-2 (Supplemental Fig. 18). From the antibody array assay, while there was increases angiogenic factors in the sine and brachial waveform treated groups, there was only a marked reduction in anti-angiogenic factors angiostatin and prolactin in the brachial E/E group. Thus, the tube formation response may reflect both a gain of pro-angiogenic factors and a loss of anti-angiogenic factors in the brachial E/E group.

We performed a proliferation assay following treatments of the cells and found that brachial waveform mechanical loading lead to increased proliferation of the MSCs after passaging the cells in polystyrene culture dishes (Supplemental Fig. 19). To examine whether the treatments led to adipogenic or osteogenic differentiation, we performed staining on the cells with Oil Red O or Alizarin Red S but did not find significant changes in the staining in comparison to static conditions (Supplemental Fig. 20). We also performed immunostaining for early markers of osteogenic and adipogenic differentiation but did not see significant changes in these with the treatments (Supplemental Fig. 21). Additionally, we grew the cells to confluence and immunostained for VE-cadherin but did not find cell-cell junctions with VE-caherin enrichment (Supplemental Fig. 22). We did however observe an overall increase in VE-cadherin in the brachial loading with E/E inhibitor group. There was no difference between the cells in terms of barrier function as measured with a permeability assay (Supplemental Fig. 23) and measurements of transepithelial electrical resistance (TEER; Supplemental Fig. 24).

Gene expression analysis by RNA-Seq demonstrates enhancement of pericyte/endothelial phenotypes and pro-angiogenic gene expression in MSCs with optimized mechanical conditioning and small molecule treatment.

To further examine whether mechanical loading/drug treatment enhanced angiogenic and pericyte-like phenotype in MSCs, we performed RNASeq on MSCs under the various treatments. A differential gene expression analysis revealed that treatment with the brachial waveform mechanical loading, with or without the ErbB/EGRB (E/E) inhibitor, significantly regulated a large number of genes in comparison to the sine wave form (Fig. 4A, B). Treatment with the E/E inhibitor also modulated a relatively large number of genes (Supplemental Fig. 25). Cells treated with brachial loading or brachial loading with E/E inhibitor treatment had similar patterns of gene expression while MSCs treated with sine or static conditions were more similar (Fig. 4C). Gene ontology analysis of the changes in the gene expression revealed significant increases in gene expression for ECM remodeling, vasculature development, and tube formation with treatment with brachial waveform loading

and brachial loading with E/E inhibitor treatment (Fig. 4D). To examine the development of a pericyte-like phenotype, we compared the gene expression of the cells in our study to the results of a gene expression analysis from another study that examined the development of pericytes and vSMCs from mesenchymal cells[47]. For brachial and brachial + E/E treated cells, there were gene expression changes consistent with a pericyte phenotype (Fig. 4E). We examined a set of genes associated with the development of endothelial phenotype[48] and found that some but not all of these genes were strongly upregulated (Supplemental Fig. 26). We also examined the gene expression for soluble factors related to angiogenesis and found increases in ANGPT2 and HGF for static + E/E inhibitor, brachial and brachial + E/E inhibitor-treated cells (Supplemental Fig. 27). To further investigate whether the brachial loading with E/E inhibitor treatment promotes differentiation of MSCs into endothelial cells or pericytes we next performed Gene Set Enrichment Analysis (GSEA) on the RNASeq datasets[49]. We found a strong enrichment of both endothelial cell and pericyte gene sets in the MSCs treated with mechanical load and mechanical load with E/E inhibitor treatment relative to the control cells (Supplemental Fig. 28).

Optimized mechanical and pharmacological conditioning of MSCs increases proangiogenic potential *in vivo*.

We next examined the effects of mechanical loading and pharmacological conditioning on the *in vivo* angiogenic properties of MSCs. We conditioned the cells with the treatments for seven days and then implanted them subcutaneously in nu/nu mice. After 14 days, there were increased numbers of vessels invading the gels implanted with MSCs exposed to brachial waveform mechanical loading based on the macroscopic images of the implant (Fig. 5A, B). In particular, the cells treated with the brachial waveform loading and pharmacological co-treatment had the highest number of large vessels invading. Analysis with laser speckle imaging revealed increased perfusion in the skin over the implants of the groups treated with the brachial waveform loaded MSCs with pharmacological co-treatment, consistent with the macroscopic appearance of the implants (Fig. 5C, D). Histological analysis of the gels also demonstrated increased cells positive for PECAM, α-SMA and double positive for PECAM/α-SMA in those treated with brachial waveform loading in combination with pharmacological inhibitor treatment (Fig. 5E, F). In addition, there were increased nestinpositive cells with brachial loading and co-treatment with the E/E inhibitor as well as cells double positive for nestin and CD146 (Fig. 5G, H). There were also marked increases in PRGFRβ and PECAM/PDGFRβ positive cells with brachial loading and co-treatment with the E/E inhibitor (Supplemental 29A, B). We assessed proliferating cells in the Matrigel using staining for Ki-67 and found that only the static cells with the co-treatment E/E inhibitor had increased numbers of proliferating cells (Supplemental Fig. 29C, D). To confirm that the cells in the Matrigel were primarily derived from the MSCs that were delivered, we performed fluorescence *in situ* hybridization (FISH) for the human X chromosome (Supplemental Fig. 30). Together, these findings support the concept that combined conditioning with pharmacological inhibitors and specific mechanical conditions can increase the pro-angiogenic properties of MSCs.

To further confirm the functional activity of the conditioned MSCs, we exposed the cells to the treatments for seven days, encapsulated them in alginate-RGD/collagen gel and

implanted them in nu/nu mice that underwent surgery to create unilaterial hind limb ischemia through femoral artery ligation. We observed enhanced recovery of perfusion in the mice treated with cells that had been conditioned with brachial waveform loading and E/E inhibitor (Fig. 5I, J). Histological analysis revealed a moderate increase in capillaries and an over two-fold increases in larger mature vessels in the muscle from mice treated with MSCs conditioned with brachial loading or brachial loading with E/E inhibitor treatment (Fig. 5K, L; Supplemental Fig. 31). We confirmed the continued presence of MSCs in the hind limb of the mice using FISH for the human X chromosome (Supplemental Fig. 32). To examine whether brachial loading and E/E treatment could work for MSCs derived from other donors, we repeated the mouse hind limb ischemia studies using MSCs from another donor (Doner 2) and measured perfusion in the legs for 28 days after induction of ischemia. We observed enhanced recovery from ischemia in mice treated with MSCs conditioned with brachial loading an E/E inhibitor from the donor as well (Supplemental Fig. 33).

Brachial waveform loading and EGFR/ErbB2–4 inhibition leads to EC/pericyte marker expression through a Yap and Smad2 mediated pathway.

From the kinase screen with mechanical load, we identified those pathways for which multiple inhibitors block the activation of p-Smad2/3 and Yap. In addition, there were many genes related to prostaglandin production/signaling were that upregulated in the RNA Seq analysis for both brachial and brachial + E/E inhibition treatment. These inhibitors included those to TrkA, TGFβR, VEGFR2, Syk, Smad2, Smad3, Yap and COX-1/2. We treated the cells with brachial + E/E inhibition and inhibitors to these pathways and then measured the signaling in the pathways using western blotting (Fig. 6A-D). In addition, we repeated these treatments and measured expression of markers for endothelial cells/pericytes by flow cytometry and production of HGF in the conditioned media of the cells (Fig. 6E, F). Combining these results with those from the kinase screen we created a hypothesized mechanistic model of the regulation of the development of the EC/pericyte through mechanical load and E/E inhibition (Fig. 7). The upregulation of HGF production was primarily controlled through a Yap mediated pathway (Fig. 6F).

Discussion

Mesenchymal stem cells are an appealing cell type for use in therapies for ischemia but clinical trials have not yielded consistent benefits for patients. The application of MSCs in vascular regeneration and tissue engineering has been limited by contradictory or inconsistent findings in studies describing MSC differentiation into vascular phenotypes[23, 26]. Using a mechanobiological screen, our studies identified conditions that enhanced MSC therapeutic activity and induced increased differentiation toward a novel phenotype with combined markers of pericytes and endothelial cells. The increased pericyte/endothelial cell-like behavior in the MSCs was supported by multiple orthogonal techniques including multi-marker flow cytometry, *in vitro* functional assays, gene expression in RNASeq and animal models. There have been several studies that support that perivascular cells may behave as MSCs in the body[40]. However, other studies suggest that pericytes are not stem cells[41]. Our study demonstrates that a hybrid pericyte-endothelial phenotype can

exist in cultured MSCs and that it can be increased through combined mechanical loading and EGFR/ErbB2–4 inhibition.

In our mechanobiological screening assays, we found conditions that had increased signaling through the p-Smad2/3 and Yap/Taz pathways. These pathways have been linked in many past studies to MSC differentiation into other MSC phenotypes[50]. However, the pathways are also important in angiogenesis and pericyte function. Signaling through Yap/Taz is enhanced in the tip cells of capillaries during angiogenesis and vascular development[51–53]. In addition, pericyte-specific knockout of Yap and Taz disrupts their coordination of alveologenesis by reducing their production of HGF[54], a soluble factor that was highly upregulated by the treatments used in our studies. Signaling through Smad2/3 is required for vascular stability[55], modulates pericyte/endothelial interactions[56] and TGF-β signaling enhances the association of pericytes/mesenchymal cells to endothelial cells[57]. There is also evidence that links Smad2/3 to endothelial differentiation in MSCs and induced pluripotent stem cells[58, 59]. In addition, Yap is localized to the nucleus in sprouting vessels and deletion of Yap and Taz causes dramatic defects in blood vessel development[53, 60]. The TGF-β pathway is key in regulating pericyte differentiation in some cell lines, regulates pericyte behavior and is important in pericyte-endothelial cell interactions[61–64]. In our study, the compounds from our high throughput screen that activated these pathways enhanced the pericyte and endothelial cell-like phenotype of the MSCs without significant increases in osteogenic or adipogenic differentiation. In addition, these treatments enhanced the expression of HGF and the angiogenic potential of the soluble factors produced by the MSCs. Our studies suggest that Yap and Smad2 signaling have a complex role in regulating MSC phenotype and regenerative properties. While our screening assays focused on activation of these pathways, future screens could target enhancement of the EC/pericyte directly and potentially achieve higher levels of enhancement of this phenotype.

Previous studies have identified that mechanical forces can increase the vascular cell phenotype of MSCs. Notably, the application of mechanical strain to MSCs increases the expression of vSMC markers[65, 66] and the application of shear stress has, in some studies, been linked to the expression of endothelial cell markers[67]. There have also been mixed results in studies aiming to induce endothelial differentiation in MSCs, with some studies finding differentiation into endothelial phenotype with VEGF-A treatment while others do not show these effects[23, 26, 68]. Our findings using flow cytometry with multiple markers suggest that there is very little pure endothelial cell differentiation of MSCs under a broad range of treatments. Given our findings of a pericyte/endothelial hybrid phenotype, even the presence of multiple endothelial markers does not exclude the possibility that the MSCs also express mural markers. Even under the most optimal conditions, only about eight percent of the total MSC population expressed endothelial markers in the absence of pericyte markers. Thus, our studies suggest that previous findings of endothelial differentiation in MSCs should be viewed with the perspective that further studies may be needed to rule out hybrid phenotypes.

In summary, our findings have identified that MSCs can be conditioned into an enhanced phenotype with increased expression of markers of pericytes and endothelial cells. The conditioning required the use of complex mechanical strain waveforms and drug treatment.

We were not able to achieve improved regenerative properties from the MSCs in the absence of applied mechanical forces. Given the wide variation in MSC behavior and loss of activity due to disease and aging, a potential approach may be to first isolate MSCs from the patient and optimize the desired phenotype using a mechanobiological screen similar to the one used in this study. For vascular regeneration, we envision that MSCs could be harvested from patients and tested in a mechanobiological screen to maximize the mixed EC/pericyte population. These mechanical and biochemical/pharmacologically optimized and conditioned cells can then be implanted or injected into the patient for treatment. Thus, while the pathways and mechanical conditions that were found to be optimal in this study may be generalizable to many MSC lines, the overall optimization process of using mechanobiological screening provides a paradigm for enhancing stem cell therapies in a patient specific manner.

Materials and Methods (Online)

Construction of a high throughput biaxial oscillatory strain system.

Mechanical strain was applied to cell culture using a high throughput system described previously[36, 38, 69]. Briefly, cells are cultured on custom made plates that are mounted on a system that applies strain. The cell culture plates were comprised of silicone membranes (0.005” thickness; Specialty Manufacturing, Inc.) that are sandwiched between two plates, with silicone rubber gaskets at the interfaces to prevent leaking. These cell culture membranes are UV sterilized and coated with 50 μg/mL fibronectin overnight at 37°C to allow cell adhesion. After cell attachment, the plates are mounted on to the top plate of the system using screws. To apply mechanical strain, a platen with 576 Teflon pistons is moved into the cell culture membrane. The motion is driven by a hygienically sealed, voice coil-type linear motor (Copley Controls). The platen is stabilized using six motion rails mounted with linear motion bearings. The hygienically sealed motor housing has chilled water running through in order to prevent over heating during operation. The 576 pistons that come in contact with the cell culture surface can be individually adjusted to have different height, allowing precise calibration of the strain applied to each well.

Cell lines and cell culture.

Human mesenchymal stem cells (Millipore, Inc.) were cultured in low glucose DMEM medium supplemented with 15% fetal bovine serum, L-glutamine and penicillin/streptomycin. Following trypsinization, cells were seeded on the membranes at 20,000 cells per cm^2 before mechanical loading. The cells were used between passages 3–6. The MSCs were derived from a donor 1 (asian male, 22 years of age), unless otherwise specified. A subset of the studies were performed using MSCs from donor 2 (white male, 24 years of age) or donor 3 (white female, 32 years of age). Fresh bone marrow cells were obtained from different donor from these cell lines (white male, 28 years of age). Human umbilical vein endothelial cell (HUVECs; PromoCell GmbH) were cultured in MCDB 131 medium supplemented with 7.5% fetal bovine serum, L-glutamine and penicillin/streptomycin and EGM-2 SingleQuot Kit (Thermo Fisher Scientific, Inc.). Human brain vascular pericytes (HBVPs) were cultured in high glucose DMEM F12 medium supplemented with 10% fetal bovine serum, L-glutamine and penicillin/streptomycin. Human aortic smooth muscle cells

(HAoSMC) were cultured in MCDB 131 medium supplemented with 10% fetal bovine serum, L-glutamine and penicillin/streptomycin. All cells were cultured in an incubator at 37 °C under a 5% CO_2 atmosphere.

Measurement of transcription factor activity.

Human mesenchymal stem cells (passage 3) were transduced with lentiviruses for the expression of luciferase reporter constructs (Qiagen) for the target transcription factors. Briefly, cells were cultured with the lentivirus (1×10^7 TU) in media containing polybrene for 24 hours. Following virus incubation, media was replaced with normal media for a day. Transduced cells were then selected with puromycin (1 μg/mL) containing media for three days. Following the treatments, the cells were lysed and the relative luminescent signal was measured using the luciferase assay kit (Promega) and read with the FlexStation-3 plate reader (Molecular Devices). For the measurement, each well was read three times and the average was taken for single data point (technical replicates). These technical replicates were averaged for biological replicates from separate wells in the data presented.

Immunocytochemical staining on silicone membranes.

Following the treatments, the cells were fixed in 4% paraformaldehyde in PBS for 10 minutes followed by washing and permeabilization with 0.1% Triton X-100 PBS for 5 minutes. Next, samples were blocked with PBS containing 5% FBS and 1% BSA for 40 minutes. After washing, cells were incubated with primary antibodies (see Supplemental Table 1 for specific antibodies and concentrations) in PBS with 1% BSA overnight at 4°C. The samples were then washed twice in PBS with 1% BSA and incubated with secondary antibodies in PBS with 1% BSA for 2 hours in a light protected environment. Cells treated with extensive washes with PBS with 1% BSA prior to mounting in anti-fade media (Vector Laboratories, Inc.). The samples were then imaged using epifluorescence microscopy (Axio Observer; Carl Zeiss, Inc.), or confocal microscopy using either an LSM 710 laser scanning confocal microscope (Carl Zeiss, Inc.) or an FV10i Confocal Laser Scanning Microscope (Olympus, Inc.).

Immunocytochemical staining on removable well plates.

Glass bottom plates with removable culture chambers (Ibidi) were coated with 8 μg/mL fibronectin in PBS for 4 hours at 37°C. Following the mechanical and chemical treatments, the cells were seeded onto the plates at a density of 50,000 cells/well and allowed to grow for two days in culture medium. Next, the cells were washed with PBS and fixed in 4% paraformaldehyde in PBS for 10 minutes followed by washing and permeabilization with 0.1% Triton X-100 PBS for 5 minutes. Next, samples were blocked with PBS containing 5% FBS and 1% BSA for 40 minutes. After washing, cells were incubated with primary antibodies (see Supplemental Table 1 for specific antibodies and concentrations) in PBS with 1% BSA overnight at 4°C. The samples were then washed twice in PBS with 1% BSA and incubated with secondary antibodies in PBS with 1% BSA for 2 hours in a light protected environment. Cells treated with extensive washes with PBS with 1% BSA prior to mounting in anti-fade media (Vector Laboratories, Inc.). The samples were then imaged

using confocal microscopy using an FV10i Confocal Laser Scanning Microscope (Olympus, Inc.).

Cell lysis and immunoblotting.

Following the treatments, the cells were lysed in 20 mM Tris with 150 mM NaCl, 1% Triton X-100, 0.1% SDS, 2 mM sodium orthovandate, 2 mM PMSF, 50 mM NaF and a protease inhibitor cocktail (Roche, Inc.). The proteins were separated on a NuPAGE 10% bis-tris midi gel (Novex) and transferred to nitrocellulose membrane using iBlot transfer stack (Novex). The membranes were blocked for one hour in 5% non-fat milk in PBS with 0.01% tween-20 (PBST). After washing twice in PBST, cells were incubated with primary antibodies (Supplemental Table 2) overnight in 1% non-fat milk at 4°C. The membranes were washed with PBST and incubated at room temperature for two hours with secondary antibody. The membrane was treated with chemiluminescent substrate (SuperSignal West Femto; Thermo Fisher Scientific, Inc.) then imaged using a digital imaging system (Cell Biosciences, Inc.).

Long term conditioning of hMSCs using biochemical factors.

For long-term conditioning, cells were incubated with the treatments as shown in Supplemental Table 3. The cells were treated with mechanical loading for 4 hours/day for 7 days under sine and brachial waveform at 0.1 Hz and 7.5% maximum strain, or cultured under static conditions. The culture media containing the treatments were replaced on day 3 and day 5 for all treatments except 5-Aza. Cells that were treated with 5-Aza had their culture media replaced after 24 hours with standard media for the rest of the experiment. In some cases, culture media was replaced with 0.5% FBS on the final day of loading to allow the harvest of conditioned media without the presence of the treatments.

Flow Cytometry.

For the separation of cells by markers of vascular phenotypes, the cells were detached from plate using Accutase (Sigma-Aldrich) and were labeled with fluorescent antibodies according the BD Bioscience flow cytometry staining kit protocol (BD 562725; see Supplemental Table 4 for the specific antibodies used). For the characterization of high passage number (Passage 6) and lentiviral transduced mesenchymal stem cells, the cells were detached from the culture plate using Accutase (Sigma-Aldrich), and were labeled with fluorescent antibodies according to the R&D Systems human mesenchymal stem cell verification flow kit protocol (R&D FMC020; see Supplemental Table 4 for the specific antibodies used). Briefly, the detached cells were centrifuged and the supernatant was removed. Fixing and permeabilizing buffer was added while the cells were vortexed and incubated for 40 min. Next, the samples were centrifuged and the supernatant was removed. Cells were then treated with washing buffer containing antibodies for 50 min. Following antibody incubation, cells were centrifuged with washing buffer two more times, before they are treated with stain buffer and measured. A BD LSR II Fortessa Flow Cytometer (BD Biosciences) was used to measure population fluorescent signals. At least 10,000 events were recorded and further gating and quantification was done through FlowJo software.

Viability flow cytometry assay.

Mesenchymal stem cells were cultured to confluence and removed from cell culture plates using 0.05% Trypsin-EDTA (Thermo Fisher). A subset of the cells was treated with 90% ethanol for 1 minute, then washed with PBS and centrifuged, in order to generate a nonviable population control. Cells were labeled with fluorescent calcein-AM and ethidium homodimer-1, following the protocol of the Live/Dead viability kit for mammalian cells (Thermo Fisher). Following fluorescent dye incubation, cells were centrifuged with washing buffer two more times, then resuspended in stain buffer. A BD LSR II Fortessa Flow Cytometer (BD Biosciences) was used to measure population fluorescent signals. At least 10,000 events were recorded and further gating and quantification was done through FlowJo software.

In vitro tube formation assay.

A day prior to tubule formation assay, growth factor reduced Matrigel (Corning, Inc.) was allowed to thaw overnight at 4°C. Human umbilical cord endothelial cells (HUVECs; passage 5) were labeled with CellTracker Red CMTPX Dye (Thermo Fisher Scientific, Inc.) and hMSCs were labeled with cell tracker green (Thermo Fisher Scientific, Inc.). These cells were then cultured in 0.5% FBS containing media for 16 hours prior to the tubule formation assay. On the day of the assay, glass bottom 96-well plates were coated with 50 μl of Matrigel per well and then incubated for 30 minutes at 37°C. The fluorescently labeled cells were passaged with the conditioned media from the long term loading onto the plates at a total seeding density of 20,000 cells/well in either hMSC alone, HUVEC alone, or a co-culture of both hMSC and HUVEC at 1:1 ratio. These cells were then imaged at 0 hour, 10 hours and 22 hours post seeding using Cytation 5 Cell Imaging Multi-mode Reader (Biotek) in the facilities of the Targeted Therapeutic Drug Discovery & Development Program (TTP) at UT Austin. For quantification, the number of complete loops formed was counted.

Measurement of soluble factor production.

Conditioned media was assayed for soluble factor production using an antibody array for angiogenic factors (Proteome Profiler Human Angiogenesis Array Kit; R&D Systems, Inc.). In addition, the concentrations of some of the factors were measured using ELISA assays per manufacturer's instructions (R&D Systems, Inc.).

Subcutaneous implantation in nu/nu mice.

All animal studies were performed with the approval of the University of Texas at Austin Institutional Animal Care and Use Committee (IACUC) and in accordance with NIH guidelines "Guide for Care and Use of Laboratory Animals" for animal care. To assess the *in vivo* response of conditioned hMSCs, the cells were implanted subcutaneously in nu/nu mice. Following seven days of conditioning with the treatments, the cells were detached using 0.05% Trypsin-EDTA and spun down at 200 g for three minutes. The supernatant was removed and the cells were resuspended in Matrigel (Corning) at 2×10^6 cells/mL, in a total volume of 200 μL. These cell suspensions were then injected subcutaneously on the dorsal surface of the six-week old nu/nu mice (Jackson Laboratories, Inc.). Blood perfusion on the

back of the mice was assessed using a custom speckle imaging system on 1, 3, 5, 7, and 14 days following implantation of cells[70]. Laser speckle imaging was quantified by taking the ratio of the perfusion in the region of skin over the implanted Matrigel to the perfusion of the skin over the sacral region of the mouse. After 14 days, the mice were euthanized and the tissue harvested for histological analysis.

Histochemical staining and immunohistochemistry of the skin tissues.

Tissues from the subcutaneous study were cryopreserved. The subcutaneous Matrigel plug was excised using a 10 mm sterile biopsy punch. The tissues were fixed in 10% formalin in PBS for 24 hours. Next, the fixed tissues were submerged in 30% sucrose in PBS for 4 days. Tissue samples were then frozen in isopentane cooled with liquid nitrogen. Frozen tissue samples were sectioned to create 20 μm thick sections. Briefly, the frozen tissue slices were incubated in PBS for 5 min. The samples were then incubated with Fc receptor blocker (Innovex Biosciences) for 30 minutes and then blocked with 25% FBS in PBS for 45 min. After two washes with 1% BSA in PBS, samples were incubated with antibodies found in **Table 5** overnight followed by secondary antibody staining for 2 hours. The antibodies used recognized both human and mouse proteins, unless otherwise specified. Samples were then mounted with Vectashield and imaged using FV10i Confocal Laser Scanning Microscope (Olympus, Inc.). For H&E staining, the frozen tissues were sectioned at 10 μm prior to staining.

Cell encapsulation in alginate beads.

The hMSCs at passage 5 were mechanically conditioned with either static, sinusoidal or brachial strain waveform at 0.1 Hz, 7.5% maximal strain for 7 days. During loading, the cells were treated with either no treatment or 1 μM EGFR/ErbB inhibitor biomolecule. The conditioned cells were then detached using 0.05% EDTA trypsin, spun down, and the supernatant removed. Approximately 1×10^6 cells were then resuspended in 200 μL alginate solution with 2% RGD peptides and 0.045% collagen. The mixture was extruded to form alginate beads with bead diameter of 1200 μm using a coaxial airflow encapsulator (Nisco Engineering AG).

Hind limb ischemia model in nu/nu mice.

To assess the angiogenic potential and the functional recovery induced by the MSCs, we performed a hind limb ischemia mice model in nu/nu mice (Jackson Laboratories, Inc.). At ten-weeks of age, the left femoral artery and branches were ligated to induce ischemia. Conditioned cells were encapsulated in alginate beads as described above and then implanted onto the ischemic leg. Blood flow through the limb was assessed using a speckle laser imaging system on day 1, 3, 5, 7, 14, and 28. The ratio between the flow though the ischemic limb to the control limb was measured to assess recovery from ischemia with correction for illumination intensity. After 28 days, the tissues were fixed using formalin perfusion and muscles of the hind limbs harvested.

RNA Sequencing and Analysis.

Following treatments, RNA was isolated from the cells from four independent wells per group using the Qiagen RNeasy Mini Kit. RNAseq was performed using an Illumina HiSeq 2500 sequencing machine. For sequencing, single reads of 50 base pairs were performed after poly-A mRNA capture using the Poly(A) Tailing Kit (Ambion) and Ultra II Directional RNA Library Prep Kit (NEB) to isolate mRNA and perform dUTP directional preparation of the mRNA library. RNA sequencing was performed by the Genomic Sequencing and Analysis Facility at UT Austin. Gene expression analysis was performed using R. Gene ontology was performed using the Molecular Signatures Database (En).

Histochemical staining and immunohistochemistry of the skin tissues.

Muscles from the ischemic tissues were first deparaffinized. Slides were then treated with antigen retrieval solution (Agilent) at 75 °C for 3 hours. Samples were then blocked with 25% FBS in PBS for 45 min. Slides were then stained for PECAM-1 using an EnVision immunostaining kit (Agilent). Briefly, samples were blocked with dual enzyme blocker solution from DAKO. Slides were then incubated with PECAM-1 antibody (ab28364; Abcam) overnight. On the following day, samples were labeled with HRP labeled secondary antibody for 30 minutes followed by extensive washes with PBS. Slides were developed with DAB chromagen for 1 minute and then counterstained using Mayer’s hematoxylin.

Fluorescence In Situ Hybridization (FISH).

Tissue slides were labeled with FISH probes following the kit instruction from VividFISH FFPE pretreatment and VividFISH CEP probe (Genecopoeia). Briefly, tissue slides were treated with pretreatment solution at 85 °C for 90 minutes followed up with a protease solution for 20 minutes. Slides were then denatured at 73 °C for 5 minutes, and treated with FISH probe mixed with the hybridization solution overnight at 42 °C. On the following day, samples were washed and treated with DAPI mounting medium. The slides were imaged using an FV10i Confocal Laser Scanning Microscope (Olympus, Inc.).

Proliferation Assay.

Following the mechanical and chemical treatments, cells were removed from the stretch plates using 0.05% Trypsin-EDTA, seeded onto optical-bottom 96 well plates at a density of 10,000 cells/well, and allowed to grow for 24 hours. Bromodeoxyuridine (5-bromo2’-deoxyuridine; BrdU) labeling solution was added to culture media. Cells were washed and stained with the detection and HRP antibodies, following the BrdU assay protocol according to the manufacturer’s instructions (Cell Signaling Technology). Absorbance was read at 450 nm using a FlexStation-3 plate reader (Molecular Devices).

Permeability Assay.

Custom steel-bottom transwell cell culture plates were built using polycarbonate membranes (Neuro Probe Inc.; #PFD3) with 3-micron pores that are sandwiched between two plates, with silicone rubber gaskets at the interfaces to prevent leaking. The membranes were UV sterilized and coated with 8 μg/mL fibronectin for 4 hours at 37°C to allow cell adhesion. After coating, the fibronectin solution was removed from the top of the transwell membranes

and warm cell culture media was added to the bottom wells of the plates. Following the mechanical and chemical treatments, cells were removed from the stretch plates using 0.05% Trypsin-EDTA (Thermo Fisher), seeded on top of the transwell membranes at a density of 50,000 cells/well, and allowed to grow for 2 days. Some wells were left unseeded to serve as the control group. Cell culture media was removed from the top of the transwell plate and replaced with 200 μL of fresh culture media containing fluorescent BSA-Texas Red (Diluted 1:10; Thermo Fisher) and 10 kDa dextran-Alexa Fluor 647 (Diluted 1:10; Thermo Fisher). 200 μL of media was subsequently removed from the bottom of the transwell plate and added to an optical-bottom 96 well plate (Thermo Fisher). Fluorescent intensity was measured using a FlexStation-3 plate reader (Molecular Devices). Culture media devoid of fluorescent additives was included in the plate reader assay to measure background fluorescent intensity.

Transepithelial electrical resistance (TEER) Assay.

Cells were conditioned with mechanical and chemical treatments and seeded into custom steel-bottom transwell culture plates as described previously. 8 transwells were left unseeded to serve as the control group. After 2 days of growth in cell culture media, the plates were removed from the 37°C CO2 cell culture incubator and allowed to cool to room temperature for 15 minutes. Electrodes from an epithelial ohmmeter (World Precision Instruments) were inserted into the bottom and top wells of the transwell plate.

Bone marrow mononuclear cell isolation.

Fresh ACD-A treated whole bone marrow was obtained from one human donor (StemExpress, Inc.). 10 mL of whole bone marrow was diluted with 5 mL of PBS without calcium and magnesium. The solution was distributed evenly amongst 4 15 mL centrifuge tubes, and 5 mL of room temperature Ficoll Paque Plus (Sigma Aldrich) was layered onto the bone marrow solution in each tube. The samples were centrifuged at 480g for 30 minutes. The resulting aqueous layer was collected, added to new centrifuge tubes and washed with PBS. This solution was centrifuged at 450g for 5 minutes and the supernatant was discarded. The cell pellet was resuspended at a density of 250,000 cells/mL and stained with flow cytometry antibodies following the protocol described previously.

Human mesenchymal stem cell functional identification.

High passage (Passage 6) MSCs were cultured as described previously. Following the protocol from the hMSC functional identification kit (R&D Systems; #SC006), cells were seeded onto glass coverslips in 24 well plates at a density of 2.1×10^4 cells/cm^2 for the adipogenic differentiation and 4.2×10^3 cells/cm^2 for the osteogenic differentiation. Cells were treated with the respectively provided differentiation media every 3 days for a total of 21 days. Following the differentiation, the cells were fixed in 4% paraformaldehyde in PBS for 10 minutes followed by washing with PBS. Next, samples were blocked and permeabilized with PBS containing 5% FBS, 1% BSA, and 0.3% Triton X-100 PBS for 40 minutes. After washing, cells were incubated with primary antibodies (see Supplemental Table 1 for specific antibodies and concentrations) in PBS with 1% BSA overnight at 4°C. The samples were then washed twice in PBS with 1% BSA and incubated with secondary antibodies in PBS with 1% BSA for 2 hours in a light protected environment. Cells treated

with extensive washes with PBS with 1% BSA prior to flipping the coverslip and mounting on glass slides in anti-fade media (Vector Laboratories, Inc.). The samples were then imaged using epifluorescence microscopy (Axio Observer; Carl Zeiss, Inc.)

Oil Red O staining.

Following the biomechanical and chemical treatments, cells were washed with PBS and fixed with 10% formalin for 30 minutes. After washing with deionized water, cells were incubated with 60% isopropanol for 5 minutes. Oil Red O stock solution (Electron Microscopy Sciences) was reconstituted in 100% isopropanol and allowed to mix for 20 minutes, following the manufacturer's protocol. The working solution was diluted 3:5 with deionized water, filtered through Whatman No.1 filter paper, added to the cells, and incubated for 20 minutes. Cells were washed until excess stain was no longer visible, and the cells were then counterstained with hematoxylin for 1 minute. Cells were washed with deionized water and imaged using light microscopy.

Alizarin Red S Staining.

Following the biomechanical and chemical treatments, cells were washed with PBS and fixed with 4% paraformaldehyde for 15 minutes. After washing with deionized water, cells were incubated with 40 mM Alizarin Red S (EMD Millipore) for 30 minutes. Cells were washed extensively with deionized water and imaged using a light microscope (Meiji, Inc.).

Gene set enrichment analysis (GSEA).

To define signature gene sets of endothelial cells, pericytes, and vascular smooth muscle cells (vSMCs), we downloaded multiple RNA-seq data sets (Supplemental Table 6). Obtained RNA-seq data sets were mapped to the human transcripts (GRCh38) with Salmon mapper (v1.1.0)[71] and the count of mapped reads was normalized as transcripts per million (TPM) using an R package of tximport (v 1.14.2)[72]. Multiple processed RNA-seq data belonging to each cell-type category were considered as replicates and compared to data obtained from mesenchymal stem cells (MSCs) using edgeR (v 3.26.8)[73] to define signature genes for each cell-type. GSEA was performed using fig 4 tool (v4.0.3)[49] with these defined gene sets (p-value 0.001, approximately 500 genes each) and the gene expression data of the brachial + E/E inhibition treated cells to control MSCs.

Endothelial and Vascular Smooth Muscle Cell Differentiation.

Human mesenchymal stem cells (Millipore, Inc.) were cultured in low glucose DMEM medium supplemented with 15% fetal bovine serum, L-glutamine and penicillin/streptomycin. Cells were seeded onto silicone membranes coated with 50 μg/mL fibronectin. Cells were treated with 50 ng/mL VEGF-A (PeproTech) to induce endothelial differentiation, or 10 ng/mL TGF-β1 (R&D Systems) and 30 μM Ascorbic Acid (Sigma-Aldrich) to induce vascular smooth muscle cell differentiation. After one week of treatment, the cells were fixed in 4% paraformaldehyde in PBS for 10 minutes followed by washing and permeabilization with 0.1% Triton X-100 PBS for 5 minutes. Next, samples were blocked with PBS containing 5% FBS and 1% BSA for 40 minutes. After washing, cells were incubated with primary antibodies (see Supplemental Table 1 for specific antibodies

and concentrations) in PBS with 1% BSA overnight at 4°C. The samples were then washed twice in PBS with 1% BSA and incubated with secondary antibodies in PBS with 1% BSA for 2 hours in a light protected environment. Cells treated with extensive washes with PBS with 1% BSA prior to mounting in anti-fade media (Vector Laboratories, Inc.). The samples were then imaged using confocal microscopy using an FV10i Confocal Laser Scanning Microscope (Olympus, Inc.).

Early osteogenic and adipogenic marker identification.

Following the biomechanical and chemical treatments, the cells were washed with PBS and fixed in 4% paraformaldehyde in PBS for 10 minutes, followed by washing and permeabilization with 0.1% Triton X-100 PBS for 10 minutes. Next, samples were blocked with PBS containing 5% FBS and 1% BSA for 40 minutes. After washing, cells were incubated with primary antibodies (see Supplemental Table 1 for specific antibodies and concentrations) in PBS with 1% BSA overnight at 4°C. The samples were then washed twice in PBS with 1% BSA and incubated with secondary antibodies in PBS with 1% BSA for 2 hours in a light protected environment. Cells treated with extensive washes with PBS with 1% BSA prior to mounting in anti-fade media (Vector Laboratories, Inc.). The samples were then imaged using confocal microscopy using an FV10i Confocal Laser Scanning Microscope (Olympus, Inc.).

Statistical analysis.

All results are shown as mean ± standard error of the mean. All experiments used biological replicates that consisted of cells in non-repeated, independent cell culture wells or tissue samples from different animals, unless specified otherwise. Multiple comparisons between groups were analyzed by two-way ANOVA followed by a Tukey post-hoc or a Dunnett post-hoc test when testing multiple comparisons versus a control group. For non-parametric data, multiple comparisons were made using the Kruskal-Wallis test followed by post-hoc testing with the Conover-Iman procedure. A p-value of 0.05 or less was considered statistically significant for all tests.

Supplementary Material

Refer to Web version on PubMed Central for supplementary material.

Acknowledgements.

The authors gratefully acknowledge funding through the American Heart Association (17IRG33410888), the DOD CDMRP (W81XWH-16-1-0580; W81XWH-16-10582) and the National Institutes of Health (1R21EB023551-01; 1R21EB024147-01A1; 1R01HL141761-01) to ABB.

References

1. Sarugaser R, Hanoun L, Keating A, Stanford WL and Davies JE. Human mesenchymal stem cells self-renew and differentiate according to a deterministic hierarchy. PLoS One. 2009;4:e6498.
2. Mao Q, Liang XL, Wu YF, Pang YH, Zhao XJ and Lu YX. ILK promotes survival and self-renewal of hypoxic MSCs via the activation of lncTCF7-Wnt pathway induced by IL6/STAT3 signaling. Gene Ther. 2019;26:165–176. [PubMed: 30814673]

3. Shi Y, Hu G, Su J, Li W, Chen Q, Shou P, Xu C, Chen X, Huang Y, Zhu Z, Huang X, Han X, Xie N and Ren G. Mesenchymal stem cells: a new strategy for immunosuppression and tissue repair. Cell Res. 2010;20:510–8. [PubMed: 20368733]

4. Shake JG, Gruber PJ, Baumgartner WA, Senechal G, Meyers J, Redmond JM, Pittenger MF and Martin BJ. Mesenchymal stem cell implantation in a swine myocardial infarct model: engraftment and functional effects. Ann Thorac Surg. 2002;73:1919–25; discussion 1926. [PubMed: 12078791]

5. Barbash IM, Chouraqui P, Baron J, Feinberg MS, Etzion S, Tessone A, Miller L, Guetta E, Zipori D, Kedes LH, Kloner RA and Leor J. Systemic delivery of bone marrow-derived mesenchymal stem cells to the infarcted myocardium: feasibility, cell migration, and body distribution. Circulation. 2003;108:863–8. [PubMed: 12900340]

6. Nagaya N, Fujii T, Iwase T, Ohgushi H, Itoh T, Uematsu M, Yamagishi M, Mori H, Kangawa K and Kitamura S. Intravenous administration of mesenchymal stem cells improves cardiac function in rats with acute myocardial infarction through angiogenesis and myogenesis. Am J Physiol Heart Circ Physiol. 2004;287:H2670–6. [PubMed: 15284059]

7. Muller-Ehmsen J, Krausgrill B, Burst V, Schenk K, Neisen UC, Fries JW, Fleischmann BK, Hescheler J and Schwinger RH. Effective engraftment but poor mid-term persistence of mononuclear and mesenchymal bone marrow cells in acute and chronic rat myocardial infarction. J Mol Cell Cardiol. 2006;41:876–84. [PubMed: 16973174]

8. Cai M, Ren L, Yin X, Guo Z, Li Y, He T, Tang Y, Long T, Liu Y, Liu G, Zhang X and Hu S. PET monitoring angiogenesis of infarcted myocardium after treatment with vascular endothelial growth factor and bone marrow mesenchymal stem cells. Amino Acids. 2016;48:81120.

9. Cai M, Shen R, Song L, Lu M, Wang J, Zhao S, Tang Y, Meng X, Li Z and He ZX. Bone Marrow Mesenchymal Stem Cells (BM-MSCs) Improve Heart Function in Swine Myocardial Infarction Model through Paracrine Effects. Sci Rep. 2016;6:28250. [PubMed: 27321050]

10. Baraniak PR and McDevitt TC. Stem cell paracrine actions and tissue regeneration. Regen Med. 2010;5:121–43. [PubMed: 20017699]

11. Cassino TR, Drowley L, Okada M, Beckman SA, Keller B, Tobita K, Leduc PR and Huard J. Mechanical loading of stem cells for improvement of transplantation outcome in a model of acute myocardial infarction: the role of loading history. Tissue Eng Part A. 2012;18:1101–8. [PubMed: 22280442]

12. Watt SM, Gullo F, van der Garde M, Markeson D, Camicia R, Khoo CP and Zwaginga JJ. The angiogenic properties of mesenchymal stem/stromal cells and their therapeutic potential. Br Med Bull. 2013;108:25–53. [PubMed: 24152971]

13. Yan J, Tie G, Xu TY, Cecchini K and Messina LM. Mesenchymal stem cells as a treatment for peripheral arterial disease: current status and potential impact of type II diabetes on their therapeutic efficacy. Stem Cell Rev. 2013;9:360–72.

14. Wagner W, Bork S, Horn P, Krunic D, Walenda T, Diehlmann A, Benes V, Blake J, Huber FX, Eckstein V, Boukamp P and Ho AD. Aging and replicative senescence have related effects on human stem and progenitor cells. PLoS One. 2009;4:e5846.

15. Kretlow JD, Jin YQ, Liu W, Zhang WJ, Hong TH, Zhou G, Baggett LS, Mikos AG and Cao Y. Donor age and cell passage affects differentiation potential of murine bone marrow-derived stem cells. BMC Cell Biol. 2008;9:60. [PubMed: 18957087]

16. Phinney DG. Functional heterogeneity of mesenchymal stem cells: implications for cell therapy. J Cell Biochem. 2012;113:2806–12. [PubMed: 22511358]

17. Du WJ, Chi Y, Yang ZX, Li ZJ, Cui JJ, Song BQ, Li X, Yang SG, Han ZB and Han ZC. Heterogeneity of proangiogenic features in mesenchymal stem cells derived from bone marrow, adipose tissue, umbilical cord, and placenta. Stem Cell Res Ther. 2016;7:163. [PubMed: 27832825]

18. Heeschen C, Lehmann R, Honold J, Assmus B, Aicher A, Walter DH, Martin H, Zeiher AM and Dimmeler S. Profoundly reduced neovascularization capacity of bone marrow mononuclear cells derived from patients with chronic ischemic heart disease. Circulation. 2004;109:1615–22. [PubMed: 15037527]

19. Hill JM, Zalos G, Halcox JP, Schenke WH, Waclawiw MA, Quyyumi AA and Finkel T. Circulating endothelial progenitor cells, vascular function, and cardiovascular risk. N Engl J Med. 2003;348:593–600. [PubMed: 12584367]
20. Li TS, Furutani A, Takahashi M, Ohshima M, Qin SL, Kobayashi T, Ito H and Hamano K. Impaired potency of bone marrow mononuclear cells for inducing therapeutic angiogenesis in obese diabetic rats. Am J Physiol Heart Circ Physiol. 2006;290:H1362–9. [PubMed: 16227342]
21. Roobrouck VD, Ulloa-Montoya F and Verfaillie CM. Self-renewal and differentiation capacity of young and aged stem cells. Exp Cell Res. 2008;314:1937–44. [PubMed: 18439579]
22. Barkholt L, Flory E, Jekerle V, Lucas-Samuel S, Ahnert P, Bisset L, Buscher D, Fibbe W, Foussat A, Kwa M, Lantz O, Maciulaitis R, Palomaki T, Schneider CK, Sensebe L, Tachdjian G, Tarte K, Tosca L and Salmikangas P. Risk of tumorigenicity in mesenchymal stromal cell-based therapies--bridging scientific observations and regulatory viewpoints. Cytotherapy. 2013;15:753–9. [PubMed: 23602595]
23. Oswald J, Boxberger S, Jorgensen B, Feldmann S, Ehninger G, Bornhauser M and Werner C. Mesenchymal stem cells can be differentiated into endothelial cells in vitro. Stem Cells. 2004;22:377–84. [PubMed: 15153614]
24. Li Q, Xia S, Fang H, Pan J, Jia Y and Deng G. VEGF treatment promotes bone marrow derived CXCR4+ mesenchymal stromal stem cell differentiation into vessel endothelial cells. Exp Ther Med. 2017;13:449–454. [PubMed: 28352314]
25. Janeczek Portalska K, Leferink A, Groen N, Fernandes H, Moroni L, van Blitterswijk C and de Boer J. Endothelial differentiation of mesenchymal stromal cells. PLoS One. 2012;7:e46842.
26. Galas RJ Jr., and Liu JC. Vascular endothelial growth factor does not accelerate endothelial differentiation of human mesenchymal stem cells. J Cell Physiol. 2014;229:90–6. [PubMed: 23794239]
27. Henderson K, Sligar AD, Le V, Lee J and Baker AB. Biomechanical Regulation of Mesenchymal Stem Cells for Cardiovascular Tissue Engineering. Advanced Healthcare Materials. 2017.
28. Homayouni Moghadam F, Tayebi T, Moradi A, Nadri H, Barzegar K and Eslami G. Treatment with platelet lysate induces endothelial differentation of bone marrow mesenchymal stem cells under fluid shear stress. EXCLI J. 2014;13:638–49. [PubMed: 26417289]
29. Bai K, Huang Y, Jia X, Fan Y and Wang W. Endothelium oriented differentiation of bone marrow mesenchymal stem cells under chemical and mechanical stimulations. J Biomech. 2010;43:1176–81. [PubMed: 20022602]
30. Dong JD, Gu YQ, Li CM, Wang CR, Feng ZG, Qiu RX, Chen B, Li JX, Zhang SW, Wang ZG and Zhang J. Response of mesenchymal stem cells to shear stress in tissue-engineered vascular grafts. Acta Pharmacol Sin. 2009;30:530–6. [PubMed: 19417732]
31. Kim DH, Heo SJ, Kang YG, Shin JW, Park SH and Shin JW. Shear stress and circumferential stretch by pulsatile flow direct vascular endothelial lineage commitment of mesenchymal stem cells in engineered blood vessels. J Mater Sci Mater Med. 2016;27:60. [PubMed: 26800691]
32. Wang H, Riha GM, Yan S, Li M, Chai H, Yang H, Yao Q and Chen C. Shear stress induces endothelial differentiation from a murine embryonic mesenchymal progenitor cell line. Arterioscler Thromb Vasc Biol. 2005;25:1817–23. [PubMed: 15994439]
33. Kinnaird T, Stabile E, Burnett MS, Shou M, Lee CW, Barr S, Fuchs S and Epstein SE. Local delivery of marrow-derived stromal cells augments collateral perfusion through paracrine mechanisms. Circulation. 2004;109:1543–9. [PubMed: 15023891]
34. Alaminos M, Perez-Kohler B, Garzon I, Garcia-Honduvilla N, Romero B, Campos A and Bujan J. Transdifferentiation potentiality of human Wharton's jelly stem cells towards vascular endothelial cells. J Cell Physiol. 2010;223:640–7. [PubMed: 20143331]
35. Tamama K, Sen CK and Wells A. Differentiation of bone marrow mesenchymal stem cells into the smooth muscle lineage by blocking ERK/MAPK signaling pathway. Stem Cells Dev. 2008;17:897–908. [PubMed: 18564029]
36. Lee J and Baker AB. Computational analysis of fluid flow within a device for applying biaxial strain to cultured cells. J Biomech Eng. 2015;137:051006.

37. Lee J, Ochoa M, Maceda P, Yoon E, Samarneh L, Wong M and Baker AB. High Throughput Mechanobiological Screens Enable Mechanical Priming of Pluripotency in Mouse Fibroblasts. https://wwwbiorxivorg/content/101101/480517v1abstract. 2018.
38. Lee J, Wong M, Smith Q and Baker AB. A novel system for studying mechanical strain waveform-dependent responses in vascular smooth muscle cells. Lab Chip. 2013;13:4573–82. [PubMed: 24096612]
39. Serrano I, McDonald PC, Lock F, Muller WJ and Dedhar S. Inactivation of the Hippo tumour suppressor pathway by integrin-linked kinase. Nat Commun. 2013;4:2976. [PubMed: 24356468]
40. Crisan M, Yap S, Casteilla L, Chen CW, Corselli M, Park TS, Andriolo G, Sun B, Zheng B, Zhang L, Norotte C, Teng PN, Traas J, Schugar R, Deasy BM, Badylak S, Buhring HJ, Giacobino JP, Lazzari L, Huard J and Peault B. A perivascular origin for mesenchymal stem cells in multiple human organs. Cell Stem Cell. 2008;3:301–13. [PubMed: 18786417]
41. Guimaraes-Camboa N, Cattaneo P, Sun Y, Moore-Morris T, Gu Y, Dalton ND, Rockenstein E, Masliah E, Peterson KL, Stallcup WB, Chen J and Evans SM. Pericytes of Multiple Organs Do Not Behave as Mesenchymal Stem Cells In Vivo. Cell Stem Cell. 2017;20:345–359 e5. [PubMed: 28111199]
42. Xie L, Zeng X, Hu J and Chen Q. Characterization of Nestin, a Selective Marker for Bone Marrow Derived Mesenchymal Stem Cells. Stem Cells Int. 2015;2015:762098.
43. Espagnolle N, Guilloton F, Deschaseaux F, Gadelorge M, Sensebe L and Bourin P. CD146 expression on mesenchymal stem cells is associated with their vascular smooth muscle commitment. J Cell Mol Med. 2014;18:104–14. [PubMed: 24188055]
44. Russell KC, Tucker HA, Bunnell BA, Andreeff M, Schober W, Gaynor AS, Strickler KL, Lin S, Lacey MR and O'Connor KC. Cell-surface expression of neuron-glial antigen 2 (NG2) and melanoma cell adhesion molecule (CD146) in heterogeneous cultures of marrow-derived mesenchymal stem cells. Tissue Eng Part A. 2013;19:2253–66. [PubMed: 23611563]
45. Wu CC, Liu FL, Sytwu HK, Tsai CY and Chang DM. CD146+ mesenchymal stem cells display greater therapeutic potential than CD146- cells for treating collagen-induced arthritis in mice. Stem Cell Res Ther. 2016;7:23. [PubMed: 26841872]
46. Bussolino F, Di Renzo MF, Ziche M, Bocchietto E, Olivero M, Naldini L, Gaudino G, Tamagnone L, Coffer A and Comoglio PM. Hepatocyte growth factor is a potent angiogenic factor which stimulates endothelial cell motility and growth. J Cell Biol. 1992;119:629–41. [PubMed: 1383237]
47. Kumar A, D'Souza SS, Moskvin OV, Toh H, Wang B, Zhang J, Swanson S, Guo LW, Thomson JA and Slukvin II. Specification and Diversification of Pericytes and Smooth Muscle Cells from Mesenchymoangioblasts. Cell Rep. 2017;19:1902–1916. [PubMed: 28564607]
48. Bhasin M, Yuan L, Keskin DB, Otu HH, Libermann TA and Oettgen P. Bioinformatic identification and characterization of human endothelial cell-restricted genes. BMC Genomics. 2010;11:342. [PubMed: 20509943]
49. Subramanian A, Tamayo P, Mootha VK, Mukherjee S, Ebert BL, Gillette MA, Paulovich A, Pomeroy SL, Golub TR, Lander ES and Mesirov JP. Gene set enrichment analysis: a knowledge-based approach for interpreting genome-wide expression profiles. Proc Natl Acad Sci U S A. 2005;102:15545–50. [PubMed: 16199517]
50. Dupont S, Morsut L, Aragona M, Enzo E, Giulitti S, Cordenonsi M, Zanconato F, Le Digabel J, Forcato M, Bicciato S, Elvassore N and Piccolo S. Role of YAP/TAZ in mechanotransduction. Nature. 2011;474:179–83. [PubMed: 21654799]
51. Sakabe M, Fan J, Odaka Y, Liu N, Hassan A, Duan X, Stump P, Byerly L, Donaldson M, Hao J, Fruttiger M, Lu QR, Zheng Y, Lang RA and Xin M. YAP/TAZ-CDC42 signaling regulates vascular tip cell migration. Proc Natl Acad Sci U S A. 2017;114:10918–10923. [PubMed: 28973878]
52. Kim J, Kim YH, Kim J, Park DY, Bae H, Lee DH, Kim KH, Hong SP, Jang SP, Kubota Y, Kwon YG, Lim DS and Koh GY. YAP/TAZ regulates sprouting angiogenesis and vascular barrier maturation. J Clin Invest. 2017;127:3441–3461. [PubMed: 28805663]
53. Neto F, Klaus-Bergmann A, Ong YT, Alt S, Vion AC, Szymborska A, Carvalho JR, Hollfinger I, Bartels-Klein E, Franco CA, Potente M and Gerhardt H. YAP and TAZ regulate adherens junction dynamics and endothelial cell distribution during vascular development. Elife. 2018;7.

54. Kato K, Dieguez-Hurtado R, Park DY, Hong SP, Kato-Azuma S, Adams S, Stehling M, Trappmann B, Wrana JL, Koh GY and Adams RH. Pulmonary pericytes regulate lung morphogenesis. Nat Commun. 2018;9:2448. [PubMed: 29934496]
55. Itoh F, Itoh S, Adachi T, Ichikawa K, Matsumura Y, Takagi T, Festing M, Watanabe T, Weinstein M, Karlsson S and Kato M. Smad2/Smad3 in endothelium is indispensable for vascular stability via S1PR1 and N-cadherin expressions. Blood. 2012;119:5320–8. [PubMed: 22498737]
56. Hirschi KK, Rohovsky SA and D'Amore PA. PDGF, TGF-beta, and heterotypic cell-cell interactions mediate endothelial cell-induced recruitment of 10T1/2 cells and their differentiation to a smooth muscle fate. J Cell Biol. 1998;141:805–14. [PubMed: 9566978]
57. Zonneville J, Safina A, Truskinovsky AM, Arteaga CL and Bakin AV. TGF-beta signaling promotes tumor vasculature by enhancing the pericyte-endothelium association. BMC Cancer. 2018;18:670. [PubMed: 29921235]
58. Di Bernardini E, Campagnolo P, Margariti A, Zampetaki A, Karamariti E, Hu Y and Xu Q. Endothelial lineage differentiation from induced pluripotent stem cells is regulated by microRNA-21 and transforming growth factor beta2 (TGF-beta2) pathways. J Biol Chem. 2014;289:3383–93. [PubMed: 24356956]
59. Ai WJ, Li J, Lin SM, Li W, Liu CZ and Lv WM. R-Smad signaling-mediated VEGF expression coordinately regulates endothelial cell differentiation of rat mesenchymal stem cells. Stem Cells Dev. 2015;24:1320–31. [PubMed: 25603382]
60. Choi HJ, Zhang H, Park H, Choi KS, Lee HW, Agrawal V, Kim YM and Kwon YG. Yes-associated protein regulates endothelial cell contact-mediated expression of angiopoietin-2. Nat Commun. 2015;6:6943. [PubMed: 25962877]
61. Shih SC, Ju M, Liu N, Mo JR, Ney JJ and Smith LE. Transforming growth factor beta1 induction of vascular endothelial growth factor receptor 1: mechanism of pericyte-induced vascular survival in vivo. Proc Natl Acad Sci U S A. 2003;100:15859–64. [PubMed: 14657382]
62. Tsukada T, Yoshida S, Kito K, Fujiwara K, Yako H, Horiguchi K, Isowa Y, Yashiro T, Kato T and Kato Y. TGFbeta signaling reinforces pericyte properties of the non-endocrine mouse pituitary cell line TtT/GF. Cell Tissue Res. 2018;371:339–350. [PubMed: 29274061]
63. Sieczkiewicz GJ and Herman IM. TGF-beta 1 signaling controls retinal pericyte contractile protein expression. Microvasc Res. 2003;66:190–6. [PubMed: 14609524]
64. Sato Y and Rifkin DB. Inhibition of endothelial cell movement by pericytes and smooth muscle cells: activation of a latent transforming growth factor-beta 1-like molecule by plasmin during co-culture. J Cell Biol. 1989;109:309–15. [PubMed: 2526131]
65. O'Cearbhaill ED, Punchard MA, Murphy M, Barry FP, McHugh PE and Barron V. Response of mesenchymal stem cells to the biomechanical environment of the endothelium on a flexible tubular silicone substrate. Biomaterials. 2008;29:1610–9. [PubMed: 18194813]
66. Jang JY, Lee SW, Park SH, Shin JW, Mun C, Kim SH, Kim DH and Shin JW. Combined effects of surface morphology and mechanical straining magnitudes on the differentiation of mesenchymal stem cells without using biochemical reagents. J Biomed Biotechnol. 2011;2011:860652.
67. Kim DH, Heo SJ, Kim SH, Shin JW, Park SH and Shin JW. Shear stress magnitude is critical in regulating the differentiation of mesenchymal stem cells even with endothelial growth medium. Biotechnol Lett. 2011;33:2351–9. [PubMed: 21805363]
68. Wingate K, Floren M, Tan Y, Tseng PO and Tan W. Synergism of matrix stiffness and vascular endothelial growth factor on mesenchymal stem cells for vascular endothelial regeneration. Tissue Eng Part A. 2014;20:2503–12. [PubMed: 24702044]
69. Lee J, Ochoa M, Maceda P, Yoon E, Samarneh L, Wong M and Baker AB. High Throughput Mechanobiological Screens Enable Mechanical Priming of Pluripotency in Mouse Fibroblasts. https://wwwbiorxivorg/content/early/2018/11/29/480517. 2018.
70. Dunn AK, Bolay H, Moskowitz MA and Boas DA. Dynamic imaging of cerebral blood flow using laser speckle. J Cereb Blood Flow Metab. 2001;21:195–201. [PubMed: 11295873]
71. Patro R, Duggal G, Love MI, Irizarry RA and Kingsford C. Salmon provides fast and bias-aware quantification of transcript expression. Nat Methods. 2017;14:417–419. [PubMed: 28263959]
72. Soneson C, Love MI and Robinson MD. Differential analyses for RNA-seq: transcript-level estimates improve gene-level inferences. F1000Res. 2015;4:1521. [PubMed: 26925227]

73. Robinson MD, McCarthy DJ and Smyth GK. edgeR: a Bioconductor package for differential expression analysis of digital gene expression data. Bioinformatics. 2010;26:139–40. [PubMed: 19910308]

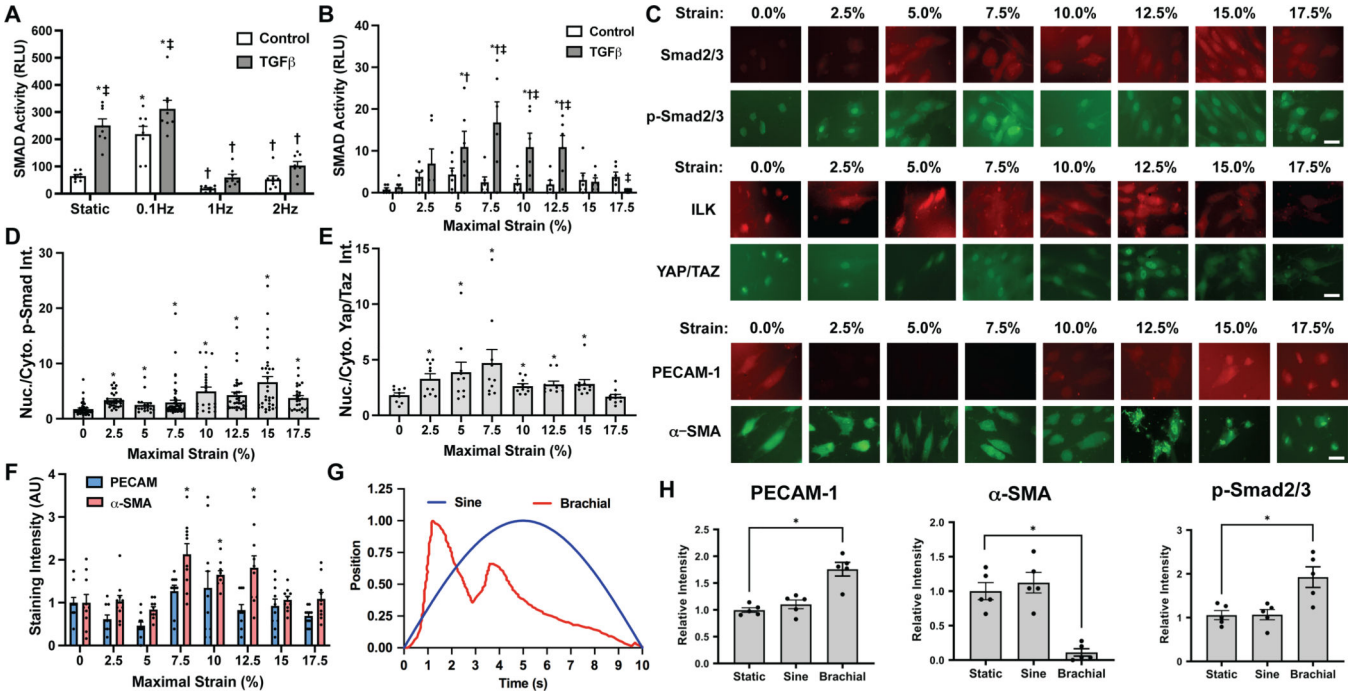

Figure 1. Specific types of mechanical stretch activate Smad2/3 and Yap/Taz pathways in mesenchymal stem cells.

(A) Transcription factor activity in MSCs was measured using a luciferase reporter assay after the application of cyclic mechanical strain (5% maximal strain) for 8 hours with co-treatment with 10 ng/ml VEGF-A or 10 ng/ml TGF-β1 (n = 8). *p = 0.001 versus static control group. †p = 0.001 versus static, growth factor treated group. ‡p = 0.024 versus control group under the same mechanical loading conditions. (B) Smad transcription factor activity in MSCs with application of load for 24 hours using the multi-strain configuration (n = 6). *p = 0.024 versus static control group. †p = 0.038 versus static, growth factor treated group. ‡p = 0.049 versus control group under the same mechanical loading conditions. (C) The MSCs were treated with mechanical load using the multi-strain format at 0.1 Hz for 24 hours and then immunostained for markers of vascular cell differentiation or signaling pathway activation. Scale bar = 100 μm. (D) Ratio of nuclear to cytoplasmic p-Smad2/3 in MSC after mechanical loading for 24 hours. *p = 0.02 versus static group. (E) Ratio of nuclear to cytoplasmic Yap/Taz in the mechanically loaded MSCs (n = 4). *p = 0.039 versus static group. (F) Quantification of PECAM and α-SMA staining in MSCS after 24 hours of mechanical loading at 0.1 Hz (n = 4). *p = 0.005 versus static group. (G) Strain waveforms for sine and brachial loading at 0.1 Hz. (H) Quantification of western blotting for vascular markers and signal activation after 24 hours of mechanical loading (n = 4). *p = 0.01 versus static and sine groups.

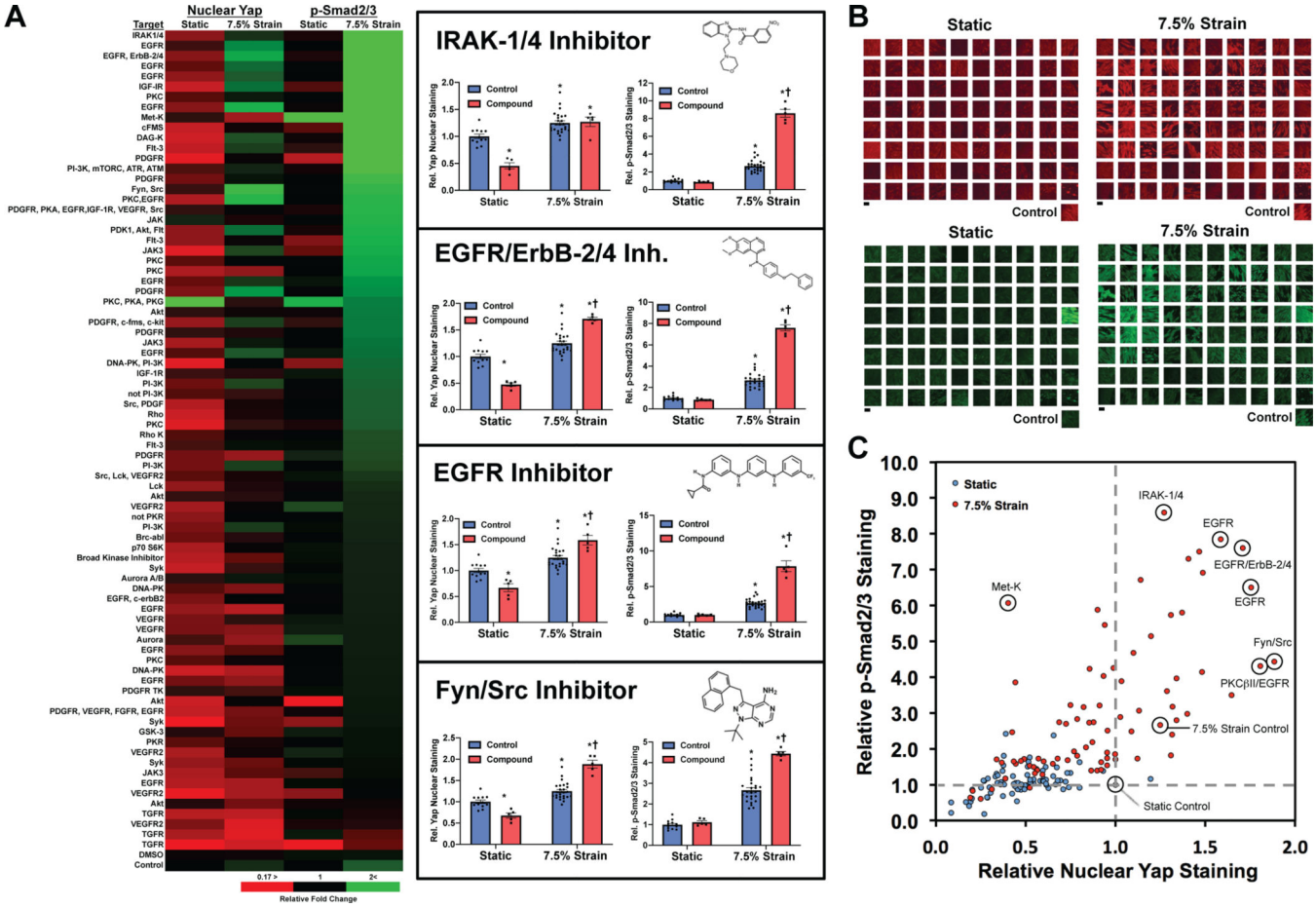

Figure 2. High throughput mechanobiological screen for small molecule inhibitors that have synergistic activation of Yap/Taz and Smad2/3 with mechanical loading.

The MSCs were treated with 7.5% mechanical strain at 0.1 Hz for 24 hours in the presence of compounds from a library of kinase inhibitors. (A) The cells were immunostained and quantified for nuclear localization of Yap/Taz and p-Smad2/3 (n = 5). *$p = 0.037$ versus cells treated with static conditions under control treatment. $^{\dagger}p = 0.001$ versus mechanically strained control group. (B) Images from immunostaining of cells arranged in the 96 well plate format. Scale bar = 50 μm. (C) Overall summary of the mechanobiological screen separated to show the response distribution for the compounds. Labeled samples indicate the target of the inhibitor used or control treatments.

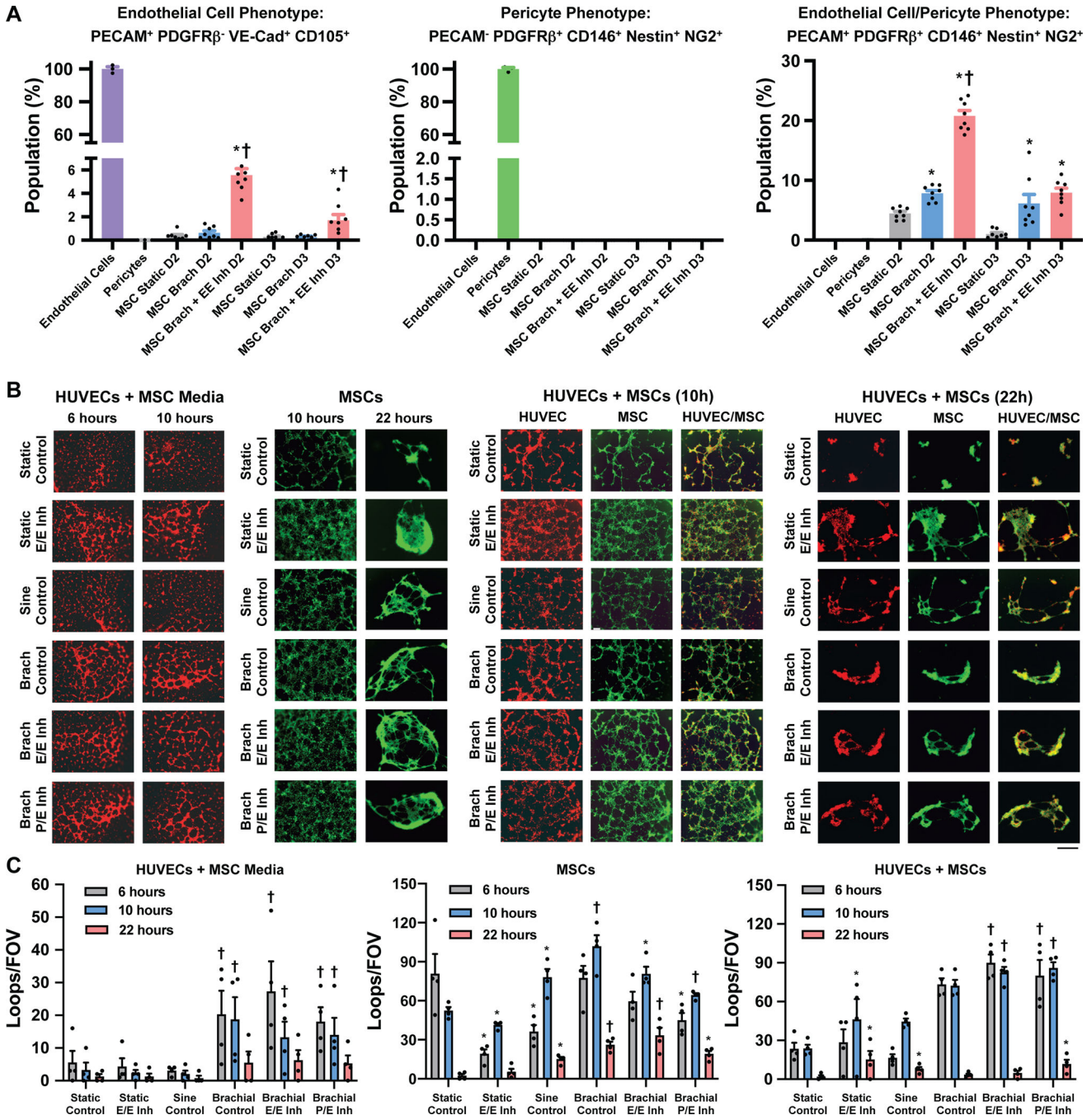

Figure 3. Biomechanical stimulation of mesenchymal stem cells with the brachial waveform and specific small molecule inhibitors leads to increased expression of endothelial cell and pericyte markers and enhanced pericyte-like activity.

(A) Analysis of cells treated with biochemical factors and/or small molecule inhibitors for seven days with 4 hours a day of mechanical loading. Cells were labeled for multiple markers of endothelial and pericyte lineage and analyzed using flow cytometry (n = 8 for MSCs; n = 3 for endothelial cells/pericytes). MSCs were derived from donor 2 (D2) or donor 3 (D3). *$p = 0.004$ versus control/non-loaded group. †$p = 0.006$ versus brachial loading group. (B) Tube formation assay analyzing the activity of the conditioned media

derived from MSCs under the treatments (HUVECs + MSC Media), the tube formation activity of the MSCs on Matrigel (MSCs), or the tube formation activity in MSCs seeded on Matrigel in co-culture with endothelial cells (HUVECs + MSCs; n = 4). *$p = 0.048$ versus static group at the same time point. MSCs were derived from donor 1. $^{\dagger}p = 0.021$ versus static and sine group at the same time point. Scale bar = 100 μm.

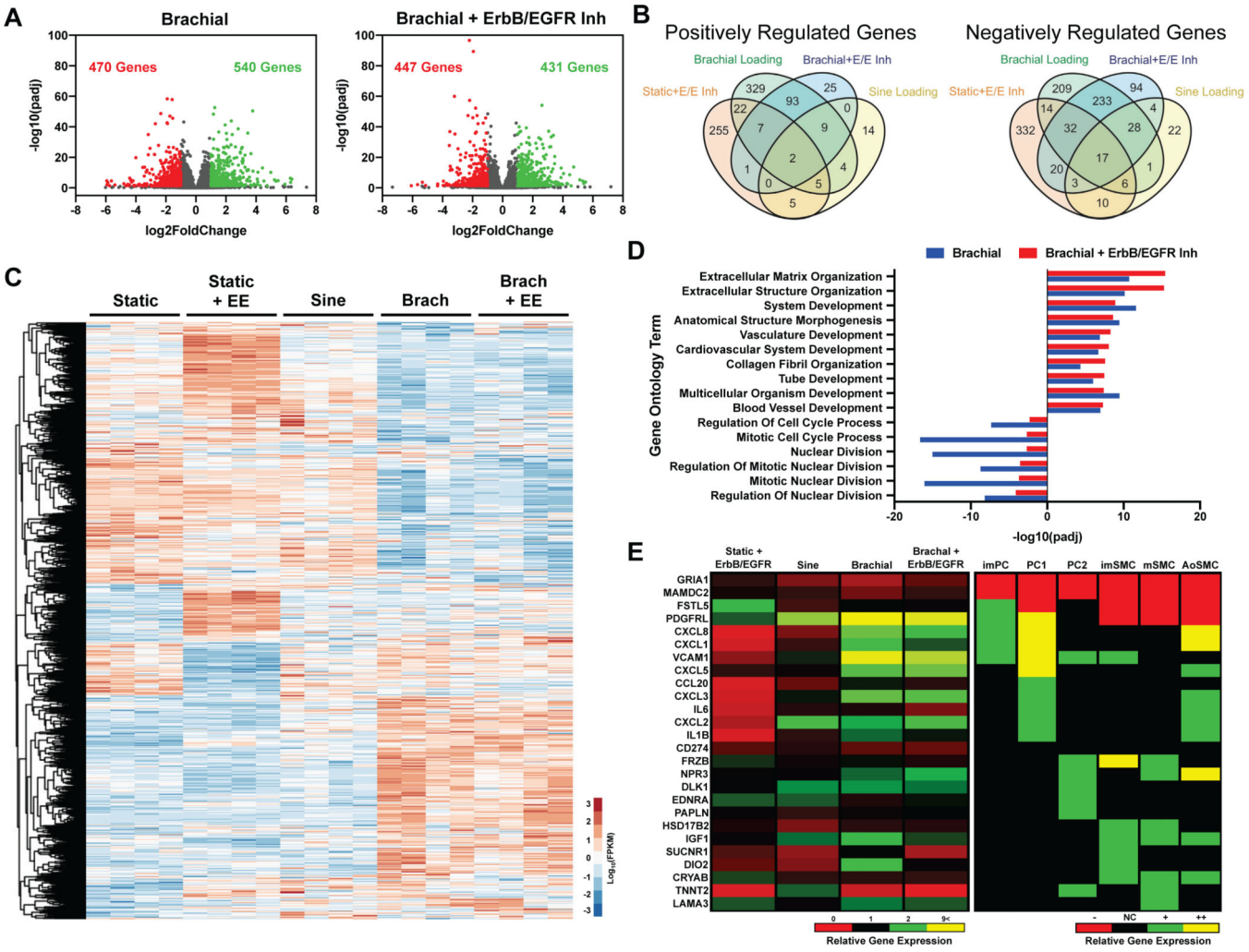

Figure 4. Gene expression analysis the RNAseq demonstrates that mechanical conditioning with brachial waveform loading enhances pericyte and endothelial cell gene expression.

MSCs were treated with mechanical load and/or an ErbB/EGFR inhibitor for seven days. (A) Volcano plots of differentiation gene expression in comparison to the static control group. (B) Venn diagrams for significantly upregulated and downregulated genes. (C) Clustering analysis of the gene expression in the MSCs for significantly regulated genes. (D) Gene ontology analysis for significantly regulated gene groups. (E) Comparison of gene expression in the treated cells to the change in gene expression in bone marrow MSCs when they differentiate into mural phenotypes.[47] The cell phenotypes listed are as follows: immature pericytes (ImPC), type 1 pericytes (PC1), type 2 pericytes (PC2), immature vascular smooth muscle cells (ImSMC), mature vascular smooth muscle cells (mSMC), and aortic vascular smooth muscle cells (AoSMC).

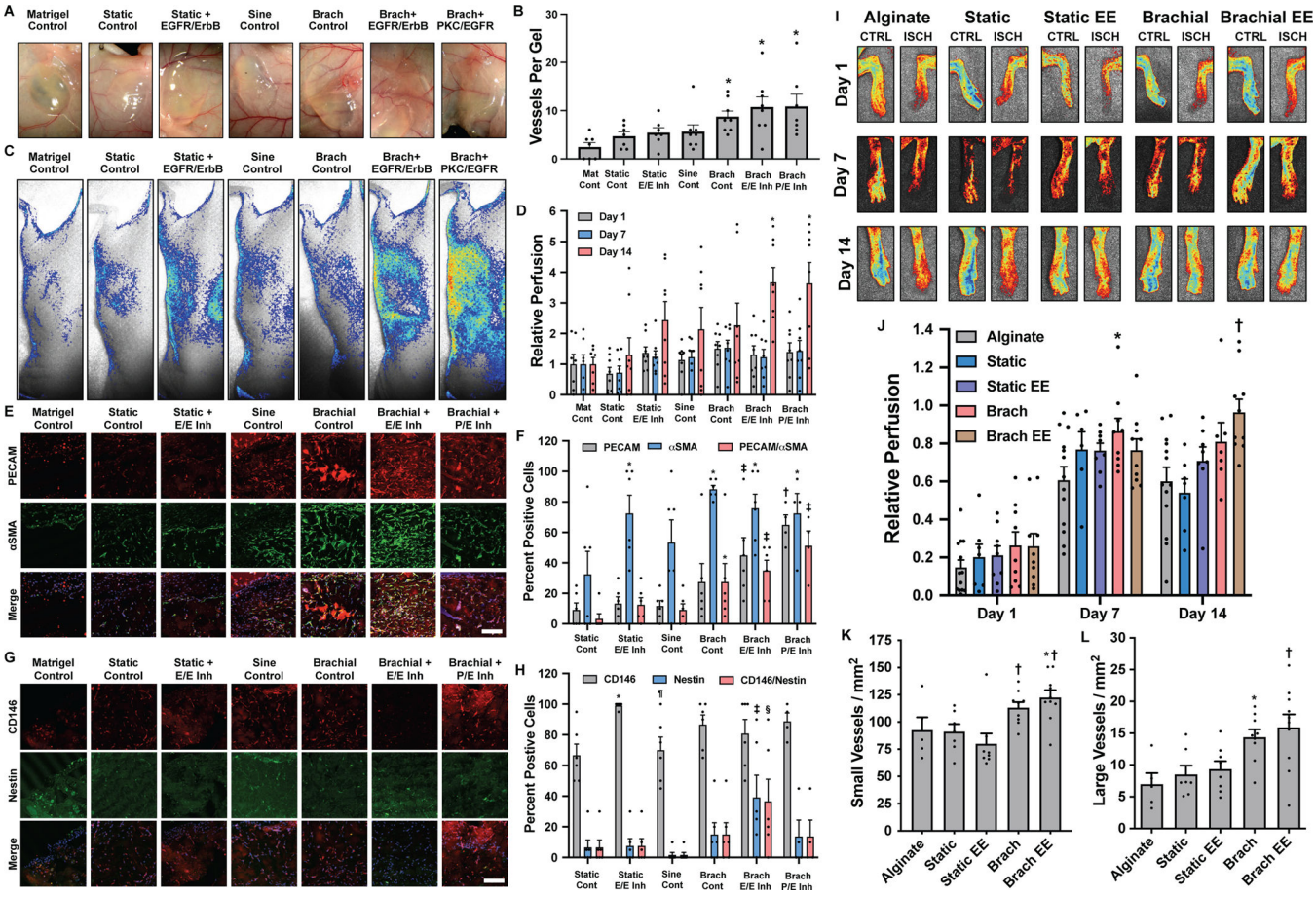

Figure 5. Optimized mechanical and pharmacological conditioning of MSCs increases their ability to induce angiogenesis and arteriogenesis following implantation subcutaneously or in a hind limb ischemia model.

The MSCs were treated under the indicated conditions for seven days in culture and then implanted subcutaneously in nu/nu mice in Matrigel. (A) Photographs of the implants after 14 days of implantation. (B) Quantification of blood vessels in the gel using macroscopic images of the gel. *$p = 0.049$ versus Matrigel, static, static with EGFR/ErbB inhibitor and sine groups (n = 6). (C) Images of laser speckle imaging of the mice after 14 days of implantation. (D) Quantification of perfusion measured by laser speckle imaging following implantation (n = 6). *$p = 0.049$ versus Matrigel and static control groups. (E) Images of tissue sections from the gel regions of the explanted tissues immunostained for PECAM and α-SMA. Scale bar = 100 μm. (F) Quantification of the percent positive cells for the indicated markers (n = 6). *$p = 0.049$ versus static control groups. $^{\dagger}p = 0.017$ versus static, static with EGFR/ErbB inhibitor, sine and brachial groups. $^{\ddagger}p = 0.021$ versus static, static with EGFR/ErbB inhibitor and sine groups. (G) Images of tissue sections immunostained for CD146 and Nestin. (H) Quantification of the percent positive cells for the indicated markers. *$p = 0.049$ versus static control groups (n = 6) $^{\dagger}p = 0.049$ versus static, static with EGFR/ErbB inhibitor, sine and brachial groups. $^{\ddagger}p = 0.049$ versus static, static with EGFR/ErbB inhibitor and sine groups. $^{\S}p = 0.044$ versus static and sine groups. $^{\P}p = 0.004$ versus static with EGFR/ErbB inhibitor group. Scale bar = 100 μm. (I) Laser speckle imaging of the

feet of mice implanted with MSCs treated for seven days with the indicated treatments. (J) Quantification of the perfusion in the feet of the mice after induction of hind limb ischemia (n = 7 for static and brachial treated groups, n = 8 for static EE treated groups, n = 10 for brachial EE treated groups, n = 13 for alginate control groups). *$p = 0.049$ versus alginate group. †$p = 0.007$ versus alginate and static groups. (K) Quantification of the number of small blood vessels in the thigh muscle of the ischemic limb in the mice implanted with MSCs conditioned with the treatments (n = 5 for alginate control groups, n = 7 for static treated groups, n = 8 for static EE and brachial treated groups, n = 10 for brachial EE treated groups). *$p = 0.042$ versus the static groups. †$p = 0.026$ versus the static EE group. (L) Quantification of large vessels in the thigh muscle of the ischemic limb of the mice (n = 5 for alginate control groups, n = 7 for static treated groups, n = 8 for static EE and brachial treated groups, n = 10 for brachial EE treated groups). *$p = 0.049$ versus the alginate group. †$p = 0.035$ versus the alginate, static and brachial EE groups.

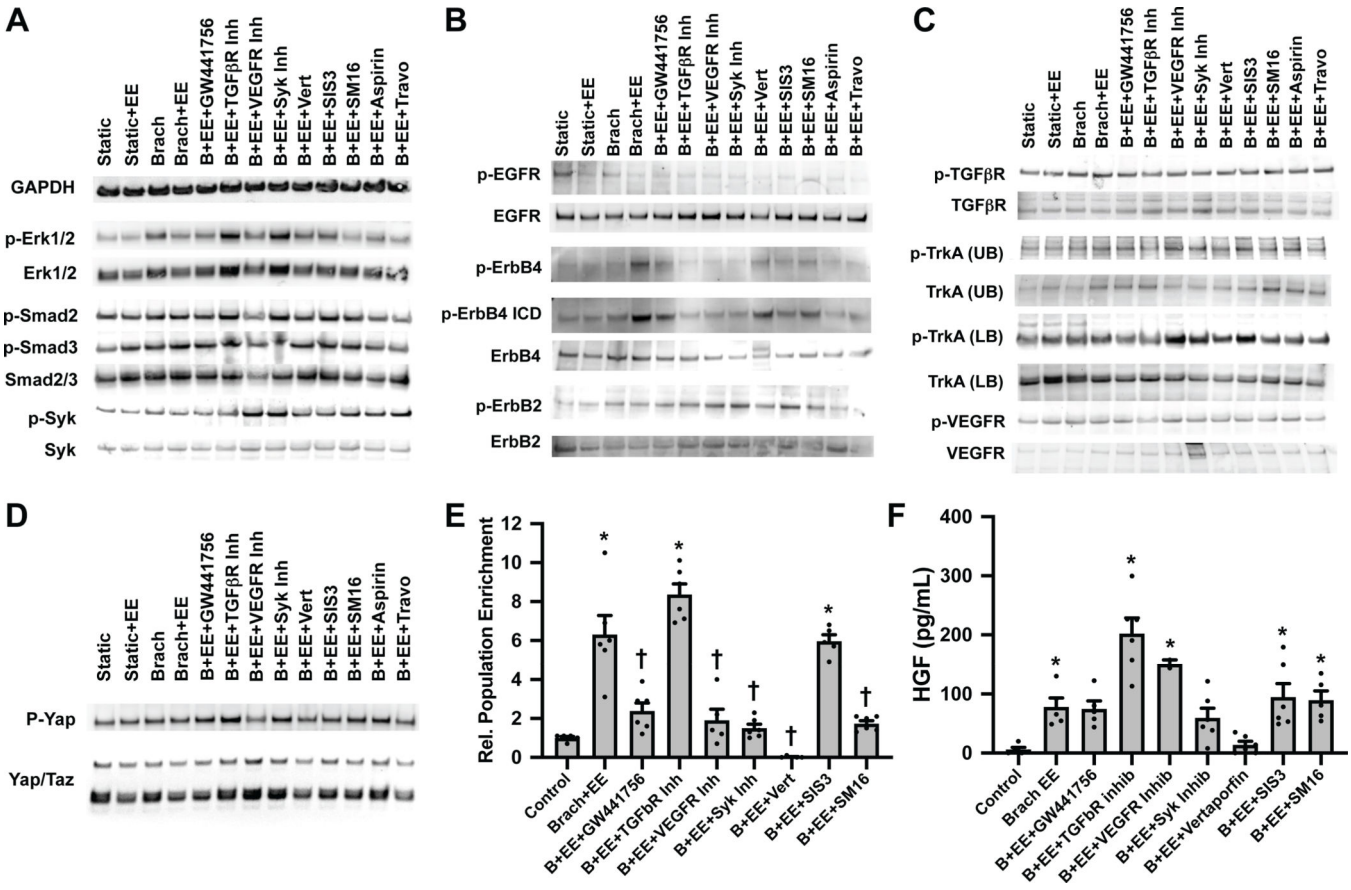

Figure 6. Analysis of cell signaling pathways activated during treatment of mesenchymal stem cells with brachial waveform loading with an EGFR/ErbB2–4 inhibitor.

(A-D) Western blotting analysis of cells after treatment with mechanical loading and EGFR/ErbB2–4 inhibitor with the addition of inhibitors as indicated. The inhibitors included a TrkA inhibitor (GW441756), TGF0βR1 inhibitor (TGFβR Inh), VEGFR2 inhibitor (VEGFR Inh), Syk inhibitor (Syk Inh), Yap inhibitor verteporfin (Vert), Smad3 inhibitor (SIS3), Smad2 inhibitor (SM16), aspirin, and prostaglandin F2α agonist travoprost (Travo). (E) Flow cytometry analysis of cells for endothelial cell/pericyte phenotype after treatment with mechanical load and inhibitors as indicated for 7 days. Endothelial cell/pericyte phenotype was defined as having the following marker expression: $PECAM^+$, $PDGFR\beta^+$, $VE\text{-}CAD^+$, $CD105^+$, $CD146^+$, $Nestin^+$ and $NG2^+$ (n = 6). $^*p = 0.001$ versus static control group. $^\dagger p = 0.001$ versus brachial EE group. (F) ELISA for production of HGF in conditioned media from MSCs treated as indicated for 7 days (n = 8). *p = 0.04 versus control group.

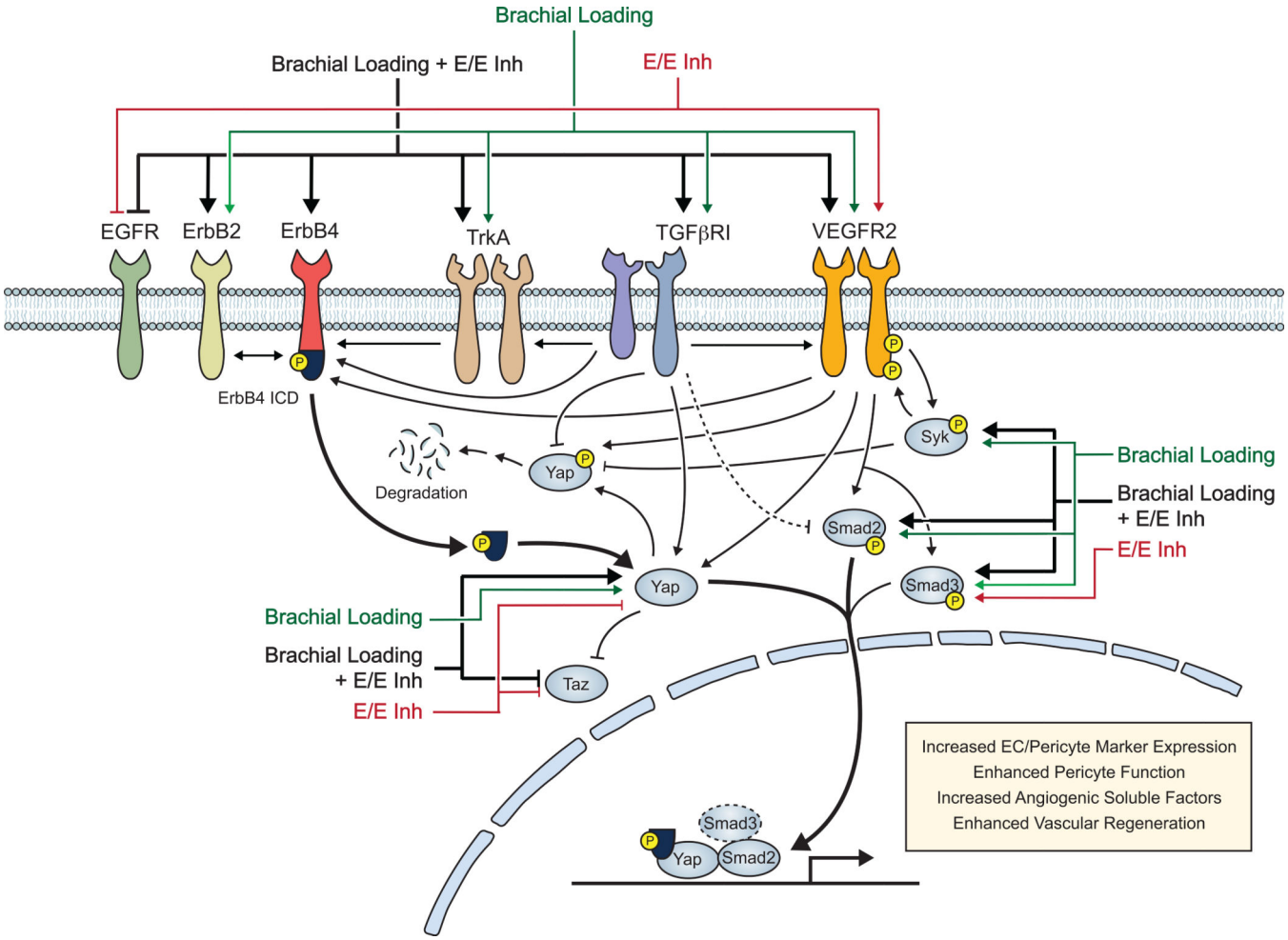

Figure 7.

Summary of hypothesized mechanism for regulating EC/Pericyte in MSCs by mechanical loading and EGFR/ErbB2–4 inhibition.